

Variations in groundwater discharge and its biogeochemical impact along a precipitation gradient

by

Breanna Waterman

B.S., Oklahoma State University, 2018

A THESIS

submitted in partial fulfillment of the requirements for the degree

MASTER OF SCIENCE

Department of Geology
College of Arts and Sciences

KANSAS STATE UNIVERSITY
Manhattan, Kansas

2020

Approved by:

Major Professor
Matthew Kirk

Copyright

© Breanna Waterman 2020.

Abstract

Groundwater discharge serves as a link between terrestrial and aquatic habitats that influences stream biogeochemistry, including nutrient availability and system stability. Climate and land use changes can alter the proportion of groundwater discharge in streamflow and impact stream biogeochemistry, but we lack a clear understanding of these relationships. Here, we consider how groundwater discharge varies with land use across Kansas precipitation gradient and the biogeochemical impacts of that variation. To assess proportions of groundwater discharge, we used hydrograph separation to analyze 15 years of continuous streamflow data from 27 streams. The calculation evaluated runoff, baseflow and baseflow index (BFI), which we used as an estimate of groundwater discharge. We evaluated stream biogeochemistry using a grab sampling approach at all sites and used a diel sampling approach at four sites. In addition, we collected groundwater samples at the diel sites. Results show that runoff and baseflow both increase with average annual precipitation ($p < 0.001$) eastward. However, the eastward increase in runoff is greater than that for baseflow. As such, the average proportion of groundwater discharge in streamflow tends to decrease eastward ($p < 0.02$). Further, groundwater discharge is influenced by watershed geology, clay content and land use to various degrees. Biogeochemistry results show that variation in major ion concentrations correlate with factors that affect groundwater discharge, such as soil and bedrock properties, as well as land use, and to a lesser extent with the calculated groundwater discharge values. Nutrients (NO_3^-/TN and NPOC) and trace elements (B, V, Ni, Co, Se, Mo, Cd) are more influenced by the proportion of agriculture than the proportion of groundwater discharge. These results highlight the significance of understanding and managing all factors that influence stream biogeochemistry for the future of water resources.

Table of Contents

List of Figures	v
List of Tables	vii
Acknowledgements.....	ix
Chapter 1 - Introduction.....	1
Chapter 2 - Methods.....	5
Study area	5
Hydrograph separation.....	7
Field methods.....	8
Geochemical analysis	10
Excess CO ₂	11
Statistical analysis.....	11
Chapter 3 - Results.....	13
Hydrograph separation results	13
Geochemical results	15
Grab sampling	15
Diel sampling results.....	18
Average diel results compared to groundwater.....	21
Chapter 4 - Discussion	24
Variability of groundwater discharge	24
Biogeochemical impact of groundwater discharge.....	26
Role of land use on groundwater discharge and stream chemistry.....	30
Limitations	32
Chapter 5 - Conclusion	34
References.....	36
Appendix A - Hydrograph Separation Results	42
Appendix B - Grab Sampling Results.....	45
Appendix C - Diel Sampling Results.....	48
Appendix D - Groundwater Data.....	56
Appendix E - WS Characteristics (Prism and GAGES II Data).....	58
Appendix F - Statistics.....	64
Appendix G - Detection Limits.....	65
Appendix H - Ferrozine Protocol.....	66
Appendix I - Extra Figures	68

List of Figures

Figure 1 Map of surficial geology across Kansas. White circles indicate co-located USGS gages and grab sampling sites. Diel sampling was conducted at the four labeled sites.....	6
Figure 2 The boxplots demonstrate the variability of the 6 hydrograph separation methods at each site from west (left) to east (right). Runoff (top) and baseflow (middle), increase eastward across the study area, whereas BFI (bottom) decreases. Precipitation generally is lower in the west and higher in the east as indicated by the fill of the boxplots.	14
Figure 3 Results of field measured parameters temperature (T), pH, dissolved oxygen (DO) and conductivity, major ions and nutrients against annual precipitation (mm/yr). Units are mg/L for everything except T (Celsius) and conductivity (mS/cm).....	16
Figure 4 Trace elements Li, B, V, Mn, Fe, Ni, Co, Cu, As, Se, Mo, and Cd concentrations (ppm, ppb or ppt) against annual precipitation (mm/yr).	18
Figure 5 Stable isotopes of water plotted against the GWML. The color of the scatter plot markers indicates whether the sample was stream water (sw) or groundwater (gw) and the shape corresponds to the site.....	22
Figure 6 Variation in groundwater (gw) and stream water (sw) concentrations of a) pH, b) conductivity, c) DO, d) Cl, e) alkalinity, f) nitrate, g) Na, h) Ca, i) NPOC. The color corresponds with site location.	23
Figure 7 Average stream BFI decreases with increased precipitation (black trend line). The color of the points corresponds with watershed clay content. Higher clay content is yellow and lower clay content is purple to blue.	25
Figure 8 Piper diagram demonstrates that water type/major ion chemistry changes from the western sites to eastern sites. The circles around each site indicates TDS. The sites are listed from furthest west at the top (Bow Creek) to the furthest east at the bottom (Blue River)..	27
Figure 9 Correlation matrix comparing stream and watershed characteristics (BFI, annual precipitation, watershed clay content and the percent agriculture or developed). Color indicates correlation (rho) and asterisks indicate statistically significant relationships.	28
Figure 10 Concentration discharge graphs for stream with high BFI value Mill Creek (0.42) compared to lower BFI value stream Mulberry Creek (0.22).....	29
Figure 11 Correlation matrix comparing streamflow components (RO, BF, BFI) to watershed characteristics (annual precipitation, and the percent agriculture or developed). Color indicates correlation (rho) and asterisks indicate statistically significant relationships.	31
Figure 12 Discharge data over the 24-hour sampling period at each stream.....	68
Figure 13 Variations in stream chemistry over 24-hour sampling period. Shaded area indicates samples taken during the night. Diel variations in field measured parameters (pH, T, DO) and calculated parameters (calcite saturation and excess carbon dioxide) are more evident at streams that do not experience large changes in discharge. NPOC at Chapman and Mill demonstrate some diel variation as seen by the peaks in concentrations near the end of the day. NO ₃ increased with decreasing discharge at Mill and Chapman. Stable isotopes of water were generally consistent during the day at Mulberry, Chapman and Mill. Mill and Chapman isotopes were slightly higher at night. Vermillion isotopes are a result of diel variations (lower during the day and higher at night).	73
Figure 14 Stream alkalinity increases with groundwater discharge (BFI). Parameters often associated with groundwater discharge (Li, Br, and CO ₂) decrease with clay content,	

possibly indicating that clay limits groundwater discharge. Cations and metals concentrations in streams also are generally lower in watersheds with higher clay content. 74

List of Tables

Table 1 Information for the well sampled near each diel sampling site is outlined below. Units for screened interval depths and distance from stream are in meters. Pumping rate is in L/min.	10
Table 2 Averages for each parameter over the course of the 24-hour sampling period at the four diel sites. Bold numbers indicate parameters that had daylight maximums and italicized numbers indicate nighttime maximums.	21
Table 3 Results of the Hydrograph Separation from USGS GW Toolbox. Results are normalized to drainage area (DA), thus units are inches/area. Streamflow components are baseflow (BF), runoff (RO) and baseflow index (BFI). This table hold results for Part and BFI standard (BFIStd).	42
Table 4 Results of the Hydrograph Separation from USGS GW Toolbox. Results are normalized to drainage area (DA), thus units are inches/area. Streamflow components are baseflow (BF), runoff (RO) and baseflow index (BFI). This table hold results for modified BFI (BFIMod) and all HySEP methods: HySEP Fixed, HySEP LocMin, HySEP Slide.	43
Table 5 Standard deviation between the six hydrograph separation analyses for each component (BF, RO, BFI). Streams with greatest standard deviation tend to occur in watersheds with higher annual precipitation values (in bold).	44
Table 6 Field measured data and major anions for grab sampling. Units are mg/L for all parameters except T (C), EC (mS), pH and alkalinity (meq/L).	45
Table 7 Major cations and nutrients data for grab sampling. Units are mg/L for all parameters except for Mn and Fe which are ppb.	46
Table 8 Trace element concentrations for grab sampling. Units for Li, B, Ni, Co, As, Se, Mo and Co are ppt. V, Cu and Zn are ppb.	47
Table 9 Field measured data and major anions for diel sampling at Mulberry Creek. Units are mg/L for all parameters except T (C), EC (mS), pH and alkalinity (meq/L).	48
Table 10 Major cations, nutrients and isotope data for diel sampling at Mulberry Creek. Units are mg/L for all parameters except isotopes, which are permille.	49
Table 11 Field measured data and major anions for diel sampling at Chapman Creek. Units are mg/L for all parameters except T (C), EC (mS), pH and alkalinity (meq/L).	50
Table 12 Major cations, nutrients and isotope data for diel sampling at Chapman Creek. Units are mg/L for all parameters except isotopes, which are permille.	51
Table 13 Field measured data and major anions for diel sampling at Vermillion Creek. Units are mg/L for all parameters except T (C), EC (mS), pH and alkalinity (meq/L).	52
Table 14 Major cations, nutrients and isotope data for diel sampling at Vermillion Creek. Units are mg/L for all parameters except isotopes, which are permille.	53
Table 15 Field measured data and major anions for diel sampling at Mill Creek. Units are mg/L for all parameters except T (C), EC (mS), pH and alkalinity (meq/L).	54
Table 16 Major cations, nutrients and isotope data for diel sampling at Mill Creek. Units are mg/L for all parameters except isotopes, which are permille.	55
Table 17 Information and field data from groundwater sampling. Measurements were taken approximately 10 minutes apart. Samples were taken after the last measurement was recorded.	56
Table 18 Average groundwater geochemical results. Units are mg/L for all parameters except T (C), EC (mS), pH, alkalinity (meq/L) and isotopes (permille).	57

Table 19 The following tables provide data gathered from online databases and used in our statistical analyses. Annual precipitation and temperature were from Prism, all other information was gathered from USGS GAGES II. Continued onto following pages. 58

Table 20 Results of spearman’s rank correlation (ρ) listed in table between site characteristics (hydrograph separation, GAGES II and Prism data) and grab sampling data. Italicized numbers represent $P < 0.05$. Bold represents $P < 0.01$. Bold and italicized represents $P < 0.005$. Land use is presented as % Ag (agriculture) and % Dev. (developed)..... 64

Table 21 Detection limits for IC. Units are mg/L. 65

Table 22 Detection limit for ICP-MS. Samples were run at 0.9-fold dilution (spiked with 10% v/v of 50 ppb Ga final concentration) as internal standard. 65

Acknowledgements

First and foremost, I'd like to thank Dr. Matt Kirk for his knowledge, eagerness to teach and learn alongside us and of course his humor – all of which were so crucial to me along this journey and a huge part of the reason I was able to get to this point. His ability to make each and everyone one of us feel like our issues and our research were his upmost priority is something I will always admire and appreciate. I would like to thank fellow students in our research group (Christina Richardson, Stephan K, Javil Hansen and Katie Andrews, Matt VP, Lucas, Gonzo and Camille) for many study sessions, hours of field and lab work help, the laughs had, and friendships made along the way. I absolutely could not have done this without all of your help - it truly takes a village.

I would like to thank members of my committee, Jesse Nippert and Walter Dodds. I am thankful for Jesse's humor and knowledge on all thing's stable isotopes and Walter for sensor/life guidance. Also, many thanks to the EPSCoR MAPS Project, specifically the aquatic group (Amy Burgin, Lydia Zeglin, Anne S, Janaeye and Alex and Justin) for helping me grow as a researcher and develop new friendships.

Last but not least, I would like to thank my support system outside of school. Thank you to my parents, Brian and Noel, for always believing in me, encouraging me, and providing me with the (frequent) comfort meal when I needed it the most. I'd like to thank my second family, the Walsh's (Emilia, Maria, Liz, and Mike) for their unconditional support. Extra special thanks to Daniel for always encouraging, and more importantly dealing with me, throughout this process.

Chapter 1 - Introduction

Groundwater discharge can provide stability by sustaining streamflow and influencing basic controls on stream habitats, such as temperature and solute loads, that directly impacts microbial activity and resulting stream biogeochemistry (Baez-Cazull et al., 2008; Barlow & Leake, 2012; Stegen et al., 2016; Jasechko, 2019). The terrestrial signature of groundwater discharge is dictated by the rate at which water percolates through and interacts with catchment soil and lithology before reaching streams (Jasechko et al., 2016; Zeglin et al., 2019). As groundwater discharges to streamflow, redox gradients are produced by bringing the terrestrially influenced, potentially reduced water to streams (Triska et al., 1993; Winter, 2001; Boano et al., 2014; Zeglin et al., 2019). The resulting interaction drives important biogeochemical processes that are essential to naturally attenuate excess nutrients and harmful pollutants that can lead to degradation of downstream water quality, eutrophication and related health risks (Diaz et al., 2004; Dubrovsky, 2010; Harvey et al., 2013; Peralta-Maraver et al., 2018).

Although previous research identifies groundwater discharge as a control for stream habitats and water quality, the consequences of climate and land-use gradients on discharge and its biogeochemical impact are unclear (Triska et al., 1993; Boano et al., 2014; Stegen et al., 2016; Peralta-Maraver et al., 2018, Cavicchioli et al., 2019). Further, previous research often focuses on small scales (i.e. hyporheic mixing); however, evidence demonstrates that these scales are hydrologically constrained and limited (Wondzell, 2011). It is important to understand these relationships as watershed and long-time groundwater discharge trends are suspected to have disproportionate influence on stream microbial communities, greenhouse gas emissions and overall water quality (Dahm et al., 1998; Jones & Mulholland 2003; Jasechko et al., 2016;

Schade et al., 2016; Stegen et al., 2016; Loecke et al., 2017; Rawitch et al., 2019; Zipper et al., 2019).

Predictions of climate change emphasize the need for an improved understanding of factors that influence groundwater discharge and stream biogeochemistry (Triska et al., 1993; Boano et al., 2014; Dodds et al., 2015; Peralta-Maraver et al., 2018; Cavicchioli et al., 2019). Regional climate predictions include the eastward shift of an established precipitation gradient (e.g. the ‘dry line’) that extends longitudinally throughout states with the United States interior (including Kansas). Shifts in the dry line will leave regions of the west of this boundary more arid and regions in the east undergoing more intense precipitation (Seagar et al., 2018). A long-term analysis of annual precipitation data demonstrates that the central and eastern portions of Kansas has already experienced greater increases in rainfall than the rest of the state (Rahmani et al., 2015; Lin et al., 2017). Changes in rainfall patterns, such as storm intensity and frequency, can influence rates of recharge, nutrient and sediment loading that can impact stream biogeochemical processes and overall water quality (Park et al., 2010; Saeger et al., 2017; Vercruyssen et al., 2017; Loecke et al., 2017).

Land-use alterations can further disrupt stream biogeochemical processes and impact water quality through increases in runoff, sediment generation, and transport of contaminants (Dahm et al., 1998; Park et al., 2010; Mulholland et al. 2008; Liu et al., 2017). Contaminants such as potentially harmful trace elements including As, Ni, Co, Mo and Cu, are particularly susceptible to mobilization from agriculture (Berrow & Ure, 1986; Indraratne & Kumaragamage, 2017). Agricultural nutrients nitrate, phosphate and organic carbon, in excess can contaminate surface and groundwater resulting in eutrophication of downstream surface waters (Domagalski et al., 2008; Richard, 2015; Foster et al., 2019; Frei et al., 2020).

The susceptibility of groundwater to anthropogenic alterations has growing implications for stream biogeochemistry and water quality (Dubrovsky, 2010; Domagalski & Johnson, 2011; Sanford & Pope, 2013). In Kansas and across the Midwest, increases in groundwater nutrient concentrations have been observed in areas of intense farming and locations with favorable geochemical conditions that allow for infiltration to the water table (Dubrovsky, 2010; Domagalski & Johnson, 2011; Richard, 2018). Groundwater transported along deeper flow paths takes years to discharge to streams, meaning the full effects of increased groundwater nutrient levels have likely not been observed (Sanford & Pope, 2013). Conversely, the infiltration of groundwater into streams can be limited by siltation, impacting biogeochemical cycling and ecosystem dynamics from microbes to macro-organisms (Jones et al., 2015). These growing trends increase the need for further research on the implications of groundwater discharge to streams.

In this study, we investigated how groundwater contribution to streams varies across a precipitation gradient and how that variation affects stream biogeochemistry. We used graphical hydrograph separation to evaluate 15 years of continuous streamflow data at 27 sites across a portion of the Kansas precipitation gradient. The analysis partitions streamflow into runoff and baseflow components, allowing us to use the proportion of baseflow out of total streamflow (BFI) as an estimate of groundwater discharge over time.

We conducted two field investigations to evaluate the influence of groundwater discharge on stream biogeochemistry: grab and diel sampling approaches. The grab sample approach was used to assess variability in stream chemistry through field measurements and analysis at the 27 streams along a portion of the Kansas precipitation gradient. The diel sampling approach was carried out at a subset of those streams to capture the daily variability of stream redox chemistry

and nutrient cycles which can vary significantly as a function of temperature, dissolved oxygen and discharge (Nimick et al., 2011). We also sampled groundwater in available wells near streams chosen for diel sampling. We utilized stream discharge, chemistry and isotopic signatures of stream and groundwater to assess the variation in stream composition over the course 24 hours. The results of this study provide insight on the impact of groundwater discharge, climate and land-use on stream biogeochemistry and water quality and has implications from municipal water-use to sustainable agriculture practices that are necessary for protecting resources, stream habitats and human health.

Chapter 2 - Methods

Study area

We surveyed the available USGS gage sites across the state that fit requirements of hydrograph separation (Barlow et al., 2015). Specifically, streams with 15 years of continuous discharge data (USGS, 2016), drainage areas less than 1295 km² (500 mi²) and groundwater discharge and surface runoff serving as main contributors to flow (Barlow et al., 2015). None of the stream sites are downstream from dams or discharges from wastewater treatment facilities. The resulting 27 sampling sites are co-located with the USGS stream gage stations from which we acquired streamflow data.

The sampling sites span a steep precipitation gradient from eastern to west-central Kansas. Along the eastern margin, annual precipitation varies northeast to southwest with annual precipitation averages of 945 mm/yr (Lin et al., 2017). From central Kansas to the extent of the western sites, annual precipitation decreases east to west with an average of 660 mm/yr (Lin et al., 2017). Reflecting this precipitation gradient, soil moisture and vegetation also change across the state with temperate deciduous forests and temperate tallgrass prairie in eastern Kansas to semi-arid grasslands in the west (Seagar et al., 2018).

Alongside the climate and vegetation gradients, elevation decreases eastward from 1231 to 207 m, creating a landscape that cuts across a range of sediments and sedimentary rocks deposited from the Paleozoic to the Cenozoic eras (Figure 1; KGS, 2008). From the western border extending into central Kansas, the predominant lithology is loess, river valley deposits and Cretaceous shale, sandstone and chalk deposits (KGS, 2008). In the eastern portion of the state, the geology is predominantly flat-lying, alternating limestone and shale of the Permian and Carboniferous systems (Stoeser et al., 2005). As a result of changes in lithology, Kansas aquifers

shift from Great Plains Aquifer sandstones and unconsolidated sand/gravel aquifers of the larger High Plains Aquifer, to limestone aquifers of the Flint Hills and Osage Aquifers in the east, to glacial drift aquifers in the northeast corner (Macfarlane et al., 2000). Alluvial aquifers are scattered across the state and tend to dominate in eastern areas that experience increased streamflow (Macfarlane et al., 2000).

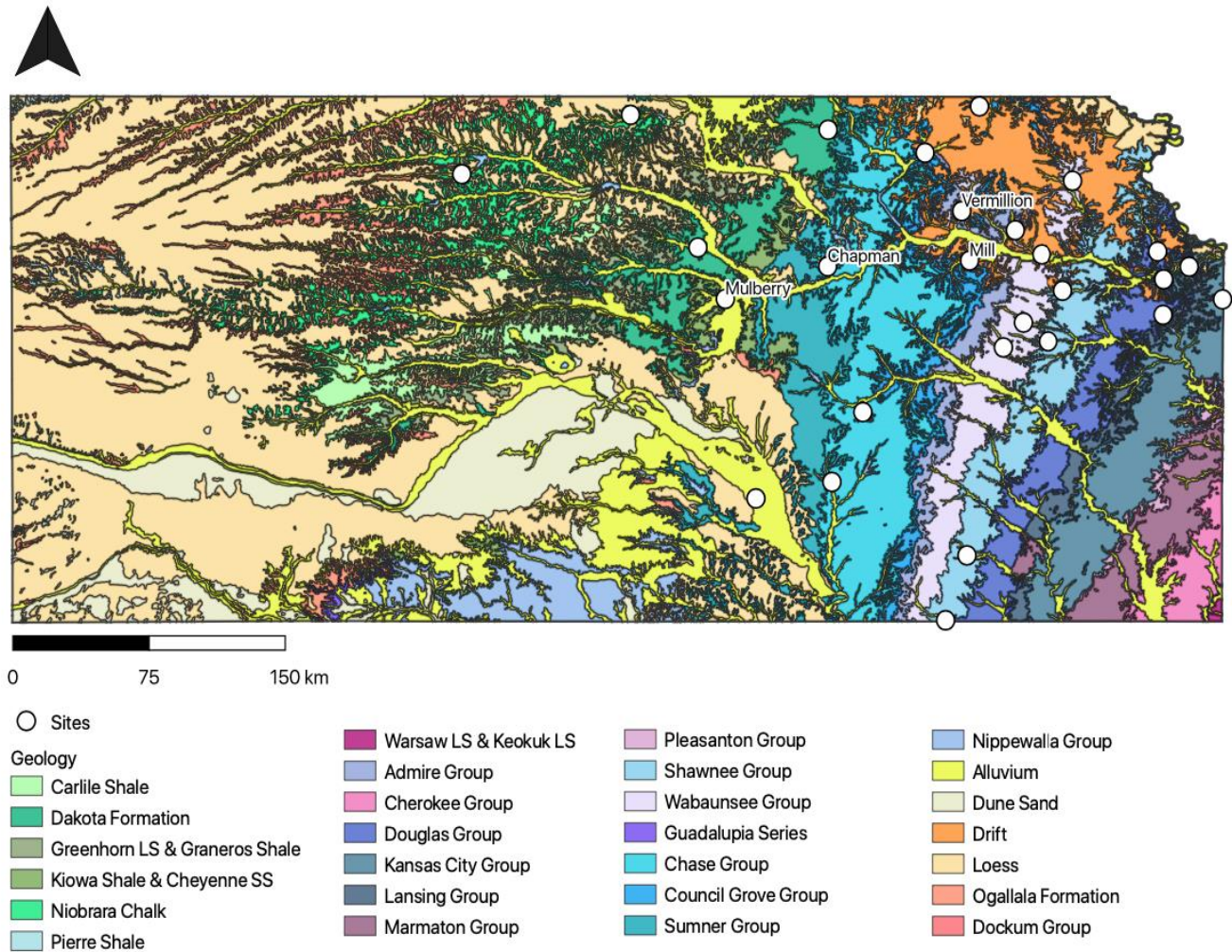


Figure 1 Map of surficial geology across Kansas. White circles indicate co-located USGS gages and grab sampling sites. Diel sampling was conducted at the four labeled sites.

Watershed characteristics were gathered from open-source, online databases. Geospatial data and watershed characteristics, such as land-use, soil type and crop coverage, were gathered

from USGS GAGES II (Falcone, 2011). Geologic map and general geology data were gathered from KGS (Stoeser et al., 2005). Average annual climate (precipitation and temperature) data were gathered from PRISM Climate Data (PRISM, 2020).

Hydrograph separation

We analyzed daily discharge data from each site with the USGS Groundwater (GW) Toolbox software (Barlow et al., 2017). The software requires daily discharge data which we acquired from the United States Geological Survey (USGS) National Water Information System for all 27 sites from 2004 to 2019 (USGS, 2016). GW Toolbox uses six different hydrograph separation methods to partition the discharge records into baseflow and runoff components: BFI standard and modified, Part, and HYSEP fixed, sliding, interval, and local minimum. A detailed description and source for each method is available in the GW Toolbox user manual (Barlow et al., 2015). Briefly, the various separation analyses partition runoff from baseflow by determining the portions of the hydrograph that are not affected by runoff via various methods (turning point factor, recession index, algorithms to connect low points, and continuous recession). We use the proportion of baseflow from total flow, known as baseflow index (BFI), as an estimate of groundwater discharge variability across Kansas.

We ran our analyses using the original settings in USGS GW Toolbox: Partition Length (N days) 5; Turning Point Test Factor (F) 0.9; Daily Recession Index (K) 0.97915. The drainage area of the basin (square miles) is required for the hydrograph separation analysis to normalize volumetric flow rates to flow rates per unit area over the contributing drainage area (in inches). Thus, the runoff and baseflow results of our analyses are in inches (volume/area). The BFI results are presented at unitless values between 0 (no baseflow component) and 1 (no runoff component).

Field methods

We used grab and diel sampling approaches to capture samples for stream biogeochemistry across a portion of the Kansas precipitation gradient. For both approaches, samples were collected at the location of the USGS stream gage. We measured water pH, temperature, and conductivity using an Oakton PC 450 meter and dissolved oxygen and atmospheric pressure using a YSI ProDO 2030 meter for all sampling approaches. We calibrated both meters each day before collecting measurements. Specific sampling approaches for each method are outlined below.

For grab sampling, we collected and filtered (0.45 μm) samples in the field for analysis of major cations and anions, trace elements, dissolved non-purgeable organic carbon (NPOC) and total dissolved nitrogen (TDN). Samples for major ions and trace elements were collected and stored in polyethylene bottles, with cation samples preserved with trace metal grade nitric acid to $\text{pH} < 2$. NPOC/TDN samples were collected and stored in amber glass bottles, preserved with concentrated hydrochloric acid to $\text{pH} < 2$. All sample vials and bottles were acid washed, pre-rinsed with de-ionized water and flushed with sample water prior to collection. Samples were stored on ice in the field until they could be transferred to the laboratory refrigerator for storage at 2 °C.

For the diel sampling approach, we selected a subset of four streams to conduct a more extensive field investigation on the effects of groundwater on stream diel biogeochemistry. We selected the streams for their similarity in size (stream order 4-5 and drainage area 780 km^2), difference in long time baseflow averages and proximity to local/domestic wells. Stream samples were collected every 1.5 hours over a 24-hour period (9 AM to 9 PM). Samples were collected for analysis of major ions, NPOC, TDN, stable isotopes of water and total phosphorus and total

iron. Major ions, NPOC and TDN were sampled, stored and preserved as outlined in grab sampling approach. Samples for stable isotopes of water were collected and stored in glass vials with neoprene seals. Unfiltered samples for total phosphorous and total iron were collected and stored in polyethylene bottles. These samples were preserved with concentrated sulfuric acid to $\text{pH} < 2$. Again, samples were stored on ice until they could be transferred to the laboratory refrigerator.

We collected groundwater samples from domestic wells that were located near the diel sites. Wells were chosen due to distance from the stream, well depth and accessibility. Samples were collected once from each well when feasible during the fall/winter season with the exception of Vermilion, which was sampled during the summer. The wells were purged prior to sampling at low-medium flow rates depending on well. Faster flow rates were due to wells having a spigot that regulated flow. General well information is located in Table 1. Groundwater pH, temperature, DO and conductivity were measured using the same probes used for stream sampling. To limit exposure to air, water was input to the bottom of 5-gallon buckets and the probes were submerged groundwater sample. The same parameters collected for diel sampling were collected for groundwater (major ions, NPOC, TDN, stable isotopes of water and total phosphorus and total iron). Groundwater samples were taken when measurements stabilized (5%) for at least three readings taken at least 10 minutes apart and collected using the same protocol outlined for stream samples.

Table 1 Information for the well sampled near each diel sampling site is outlined below. Units for screened interval depths and distance from stream are in meters. Pumping rate is in L/min.

Site	Lat./ Long.	Well Depth	Static Water Level	Interval Depths	Sed/rock type	Distance from Stream	Pumping Rate
Vermillion	39.347, -96.22	60'	14'	7.6 – 12.2 17.7 –18.3	Loose cherty limestone/ limestone	214	22.27
Chapman	39.028, -97.047	38'	7'	5.5- 11.6	Fine sand, loose coarse rock	647	0.5
Mill	39.072, -96.166	48'	16'	13.1- 14.6	Chert gravel	806	17.47
Mulberry	38.844, -97.685	65'	17'	17.7 –18.9	Sand & gravel	62	19.82

Geochemical analysis

The geochemical analyses were primarily conducted in the biogeochemical laboratory in the Kansas State University Department of Geology. We measured alkalinity using Gran alkalinity titrations with 0.02 N sulfuric acid titrant. We measured major ion concentrations using a Thermo Fisher Scientific ICS-1100 Ion Chromatograph (IC). NPOC and TN were measured using Shimadzu total organic carbon analyzer using the NPOC/TN analysis method. The total phosphate and total iron from diel sampling were measured by direct colorimetric analysis using Thermo Scientific Genesys 10S UV-Vis spectrophotometer. We measured total phosphate following the USEPA 365.3/1 total orthophosphate method and total iron using the ferrozine method (Stookey, 1970). Major cations and trace elements were measured at the RBC Spectroscopic and Biophysics Core Facility, University of Nebraska using an Agilent ICP-MS Model 7500 cx. Standards and quality control samples were used in all analyses.

We used water stable isotopes ($\delta^{18}\text{O}$ and δD) to evaluate contribution of groundwater to streams at diel sites. The isotopic abundance for a sample is expressed in δ notation as parts per mil (‰) according to:

$$\delta = [(R_{\text{sample}}/ R_{\text{std}}) - 1] \times 1000 \quad (1)$$

where R_{sample} and R_{std} are the abundance ratios of heavy to light isotopes for the sample and standard (Vienna standard mean ocean water), respectively. Stable isotopes of water were analyzed on L2130-I Picarro isotope and gas concentration analyzer in the Stable Isotope Mass Spectrometry Laboratory in the Division of Biology at Kansas State University.

Excess CO₂

We estimated excess CO₂, a measure of the potential for CO₂ loss, by comparing the concentration of dissolved CO₂ in the streamwater (CO_2^{sample}) to the concentration that would be present if the water were in equilibrium with the atmosphere CO_2^{equilib} (Rawitch, 2019):

$$\text{excess } CO_2 = \frac{CO_2^{\text{sample}}}{CO_2^{\text{equilib}}} \quad (2)$$

We calculated CO_2^{sample} concentrations from measured sample chemistry using The Geochemist's Workbench software (version 12; Bethke, 2010) and estimated CO_2^{equilib} concentrations using Henry's law. For our estimate of CO_2^{equilib} , we assumed an atmospheric CO₂ partial pressure of 4.1185×10^{-4} atm and adjusted the value of the Henry's law constant ($3.4\text{E-}2$ at 25°C ; Sander, 1999) based on the temperature measured in the field for the sample and the van't Hoff equation.

Statistical analysis

We tested the statistical relationships within our data using RStudio, version 1.2.5033 (RStudio Team, 2019). Spearman's Rho rank order correlation test was used to assess the

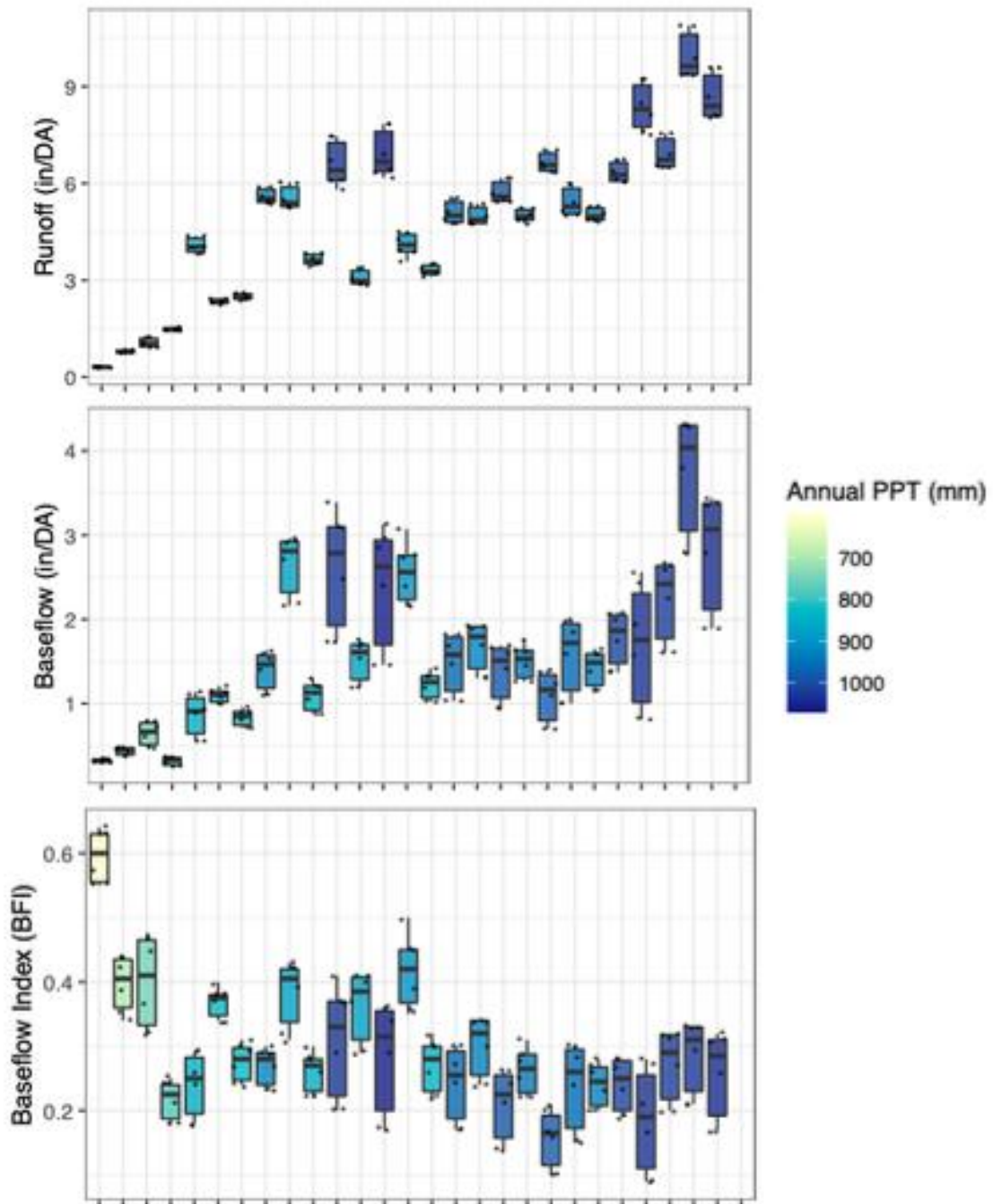
strength of variability between our parameters. We used a threshold for significance of correlation (ρ) greater than 0.40 and probability value (P) less than 0.05.

Chapter 3 - Results

Hydrograph separation results

Runoff and baseflow increase eastward across the study area in the direction of increasing precipitation (west to east). The increase in runoff (0.3 to 9.96 in) across the study area was greater than that for baseflow (0.32 to 3.72 in). As a result, BFI generally decreased westward across the study area (0.6 to 0.26). For example, Salt Creek near Ada (western site) had an average of 0.64 inches in baseflow with 1.71 inches of total flow. Kill Creek (eastern site) had an average of 2.79 inches of baseflow and 12.46 inches of total flow. Despite Kill Creek having a higher amount of baseflow, Salt Creek had a higher proportion of baseflow out of total streamflow.

The results of the hydrograph separation analyses were similar at each site and demonstrated consistent trends across the study area. The variability between the six different hydrograph separation methods for each component (runoff, baseflow and BFI) at each site can be observed in Figure 2. The greatest variation in results were observed at streams that have higher annual precipitation (Figure 2 and Table 5). The full results are available in Table 3 and Table 4 in Appendix A. We used the average from all six hydrograph separation methods to compare our hydrograph separation results to all other data (watershed characteristics, geochemical results, etc.).



W E

Figure 2 The boxplots demonstrate the variability of the 6 hydrograph separation methods at each site from west (left) to east (right). Runoff (top) and baseflow (middle), increase eastward across the study area, whereas BFI (bottom) decreases. Precipitation generally is lower in the west and higher in the east as indicated by the fill of the boxplots.

Geochemical results

Grab sampling

Results of our geochemical analysis reveal considerable variation in streamwater chemistry across the precipitation gradient (Figure 3). Stream temperature, DO and pH showed inconsistent trends across the study area. Temperature ranged between 2 and 8 °C. Stream pH values generally ranged from 8 and 8.75, with a minimum value of 6.92 and a maximum of 9.46. Dissolved oxygen in streams ranged from 11.6 to 20.3 mg/L, yet most values fell between 12 and 15 mg/L.

Conductivity, bromide and chloride follow similar trends to each other, with higher concentrations on the western and eastern ends of the precipitation gradient than in the middle. Stream conductivity ranged from 0.5 to 2.17 mS, with average value of 0.87 mS. Stream bromide concentrations ranged from below detection (0.06 mg/L) to 3.29 mg/L with an average of 1.3 mg/L. Average chloride concentrations were 63.5 mg/L, with concentrations varying significantly from 6.5 up to 395.6 mg/L.

Concentrations of other major ions (sulfate, alkalinity, fluoride, sodium, potassium, calcium and magnesium) generally decreased with precipitation. Sulfate concentrations ranged from 20 up to 256.2 mg/L. The alkalinity ranged from 3.63 to 8.17 meq/L. Fluoride concentrations ranged from 0.17 to 0.4 mg/L. Sodium concentrations ranged from 6 up to 214 mg/L. The concentrations of potassium ranged from 1 to 6 mg/L. Calcium concentrations ranged from 47.4 to 114 mg/L. Magnesium varied between from 5.8 to 26 mg/L.

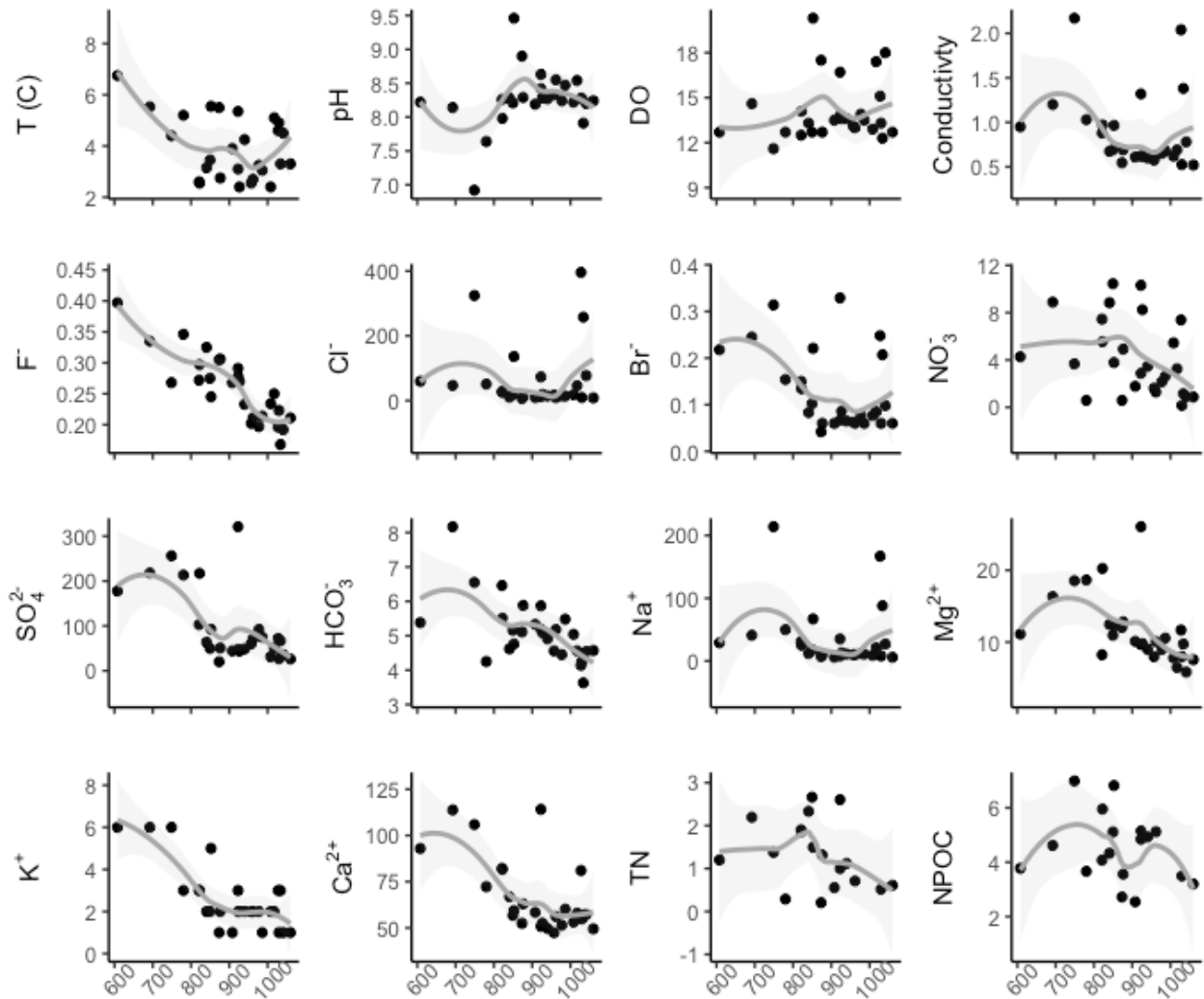


Figure 3 Results of field measured parameters temperature (T), pH, dissolved oxygen (DO) and conductivity, major ions and nutrients against annual precipitation (mm/yr). Units are mg/L for everything except T (Celsius) and conductivity (mS/cm).

Nutrients nitrate, TDN and NPOC, also generally did not demonstrate observable trends with precipitation across the study area. Only 18 sites were analyzed for TDN and NPOC. Nitrate and TDN had minimums and maximums at the same locations, from 0.59 to 10.45 mg/L and 0.21 to 2.66 mg/L, respectively. NPOC ranged from 2.55 to 6.99 to mg/L, again with no

consistent trend across the sites. Phosphorous concentrations generally decreased as precipitation increased from 2 to below 0 mg/L (not shown).

Trace elements lithium, boron, vanadium, arsenic, molybdenum and selenium also tended to decrease in concentration with increasing precipitation (Figure 4). Lithium concentrations decreased from 39,011 to 719 ppt, with the majority of streams having concentrations below 20,000 ppt. The average stream boron concentrations were 22,096 ppt and ranged from 72,652 to 8,335 ppt. Stream vanadium concentrations were 6 ppb at western sites and decreased to below 1 ppb as precipitation increased. Arsenic and molybdenum decreased from 3,779 to 343 ppt and 5,387 to 78 ppt, respectively. Selenium concentrations ranged from 7,972 to 149 ppt, with higher concentrations in areas of lower precipitation.

Trace elements iron, manganese, cobalt, nickel, copper, zinc and cadmium did not demonstrate such trends (Figure 4). Average stream iron and manganese concentrations varied from site to site, ranging from 2 to 77 ppb and from 10 up to 347 ppb respectively. Stream zinc, cadmium and copper concentrations for most streams were below 30 ppb, 50 ppt and 2 ppb respectively, with the exception of outliers (Mill Creek at Washington for Zn, Mulberry and Chapman Creeks for Cd and Vermillion Creek for Cu). Nickel and cobalt (not shown) concentrations ranged from below detection to 1,921 ppt and 69 to 609 ppt, respectively.

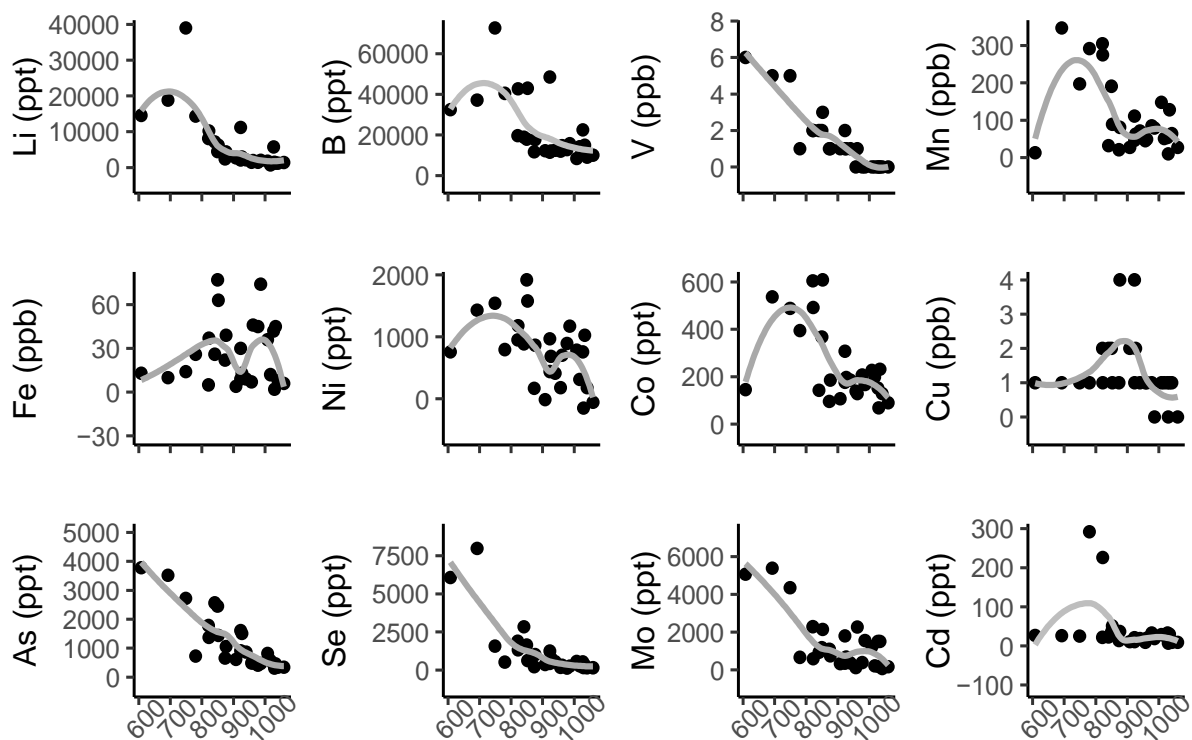


Figure 4 Trace elements Li, B, V, Mn, Fe, Ni, Co, Cu, As, Se, Mo, and Cd concentrations (ppm, ppb or ppt) against annual precipitation (mm/yr).

Diel sampling results

Results of our diel geochemical analysis show that stream biogeochemistry not only varies across sites, but also demonstrates variability throughout the day. Average stream measurements and concentrations from the 24-hour sampling period are available in Table 2. Full results are available in the appendix (Diel Sampling Results; Extra Figures).

In general, streamflow decreased gradually over the sampling period. Discharge decreased the most at Mill Creek (360 to below 300 cfs), followed by Chapman (105 to below 85 cfs), then Mulberry Creek (23 to 21 cfs). Although discharge at Vermillion Creek generally decreased over the sampling period, there was a peak in discharge that occurred during the day before concentrations then decreased over the rest of the sampling period.

Stream water temperature and DO increased during the day and decreased at night. The variation in temperature over the sampling period was greatest at Vermillion Creek (24.1 to 29.3 °C) and least at Mill (24 to 25.4 °C). The variation in DO was greatest at Vermillion again (6.6 to 11.8 mg/L) and was lowest at Chapman Creek (6.8 to 7.4 mg/L).

Stream pH and conductivity were more variable from site to site. Stream pH increased during the day at Vermillion and Mulberry Creeks, ranging from 8.21 to 8.35 and 8.06 to 8.2 respectively. Conversely, pH at Mill Creek was lower during the day and higher at night and ranged from 8.08 to 8.19. Chapman Creek pH and conductivity both increased over the sampling period, from 7.89 to 8.04 and from 0.67 to 0.81 mS/cm respectively. Mulberry Creek conductivity also increased from 1.07 to 1.086 over the sampling period. Conductivity was generally consistent at Mill Creek yet did experience a slight increase from 0.59 to 0.61. Vermillion Creek was an exception, with conductivity decreasing during the day (from 0.67 to 0.62 mS/cm) and increasing at night (0.62 to 0.66 mS/cm).

Stream excess CO₂ followed a trend that was opposite of pH at all sites. At Vermillion and Mulberry Creeks, excess CO₂ decreased during the day and increased at night with a range of 2.12 and 2.79 (unitless) respectively. Excess CO₂ at Mill Creek was higher during the day and lower at night and ranged from 4.7 to 6.58. At Chapman Creek, excess CO₂ decreased over the sampling period from 8.97 to 6.18.

Trends in major ions concentrations also varied based on site. Chloride concentrations generally increased at Mill (7.89 to 10.59 mg/L), Chapman (15.58 to 19.326 mg/L) and Mulberry Creeks (57.25 to 61.61 mg/L). Conversely, Vermillion chloride concentrations generally decreased from 15.25 to below 13.36 mg/L. Nitrate concentrations increased at Mill (5.13 to 5.81 mg/L) and Chapman (5.48 to 6.52 mg/L) Creeks. Nitrate at Vermillion Creek decreased from

5.71 mg/L in the morning to 4.55 mg/L in the evening and slightly increased during the night to 5.04 mg/L. Nitrate at Mulberry was fairly consistent and ranged from 1.7 to 1.97 mg/L. Calcium generally increased over the 24-hour period at Mill, Chapman and Mulberry Creeks. Calcium concentrations at Vermillion decreased during the day from 84.56 to 77.24 mg/L and increased through the night to 82.47 mg/L. Magnesium concentrations at Mill and Chapman generally increased over the study period from 16.73 to 17.67 mg/L and 44.67 to 52.95 mg/L. Vermillion magnesium concentrations did not demonstrate a clear trend and varied slightly from 23.13 to 23.74 mg/L. Magnesium at Mulberry Creek was generally higher during the day and lower at night and ranged from 29.9 to 30.53 mg/L.

Again, TDN and NPOC trends differed from site to site. Mill, Vermillion and Chapman Creeks were consistent over the sampling period with a range of 0.17, 0.36 and 0.58 mg/L respectively. Mulberry generally decreased from 1.26 to 0.80 mg/L over the sampling period. NPOC concentrations at Mill Creek peaked in the evening (3.26 mg/L) but was lowest during the middle of the day and middle of the night (2.23 and 2.13 mg/L respectively).

Stable isotopes of water $\delta^{18}\text{O}$ and δD were consistent during the day at Mill, Chapman and Mulberry Creeks. Mill and Chapman Creek isotopes slightly increased during the night. Stable isotopes were the most variable at Vermillion Creek, where they decreased during the day to -4.9 ‰ and increased during the night to -2.3 ‰ for $\delta^{18}\text{O}$. The trend for δD was the same, with values ranging from -32 to -24 ‰.

Table 2 Averages for each parameter over the course of the 24-hour sampling period at the four diel sites. Bold numbers indicate parameters that had daylight maximums and italicized numbers indicate nighttime maximums.

Parameter	Mill	Vermillion	Chapman	Mulberry
Q (cfs)	328.8	26.24	92.02	21.74
T (C)	24.74	26.55	21.23	26.12
pH	<i>8.15</i>	8.27	<i>7.97</i>	8.13
EC (mS)	0.6	0.65	0.74	1.084
DO (mg/L)	7.45	8.49	7.07	7.09
Cl (mg/L)	8.43	14.33	17.38	59.64
Br (mg/L)	0.05	0.09	0.11	0.19
NO ₃ (mg/L)	<i>5.57</i>	<i>5.06</i>	<i>6.01</i>	1.84
Na (mg/L)	8.64	18.39	27.6	76.65
K (mg/L)	3.16	3.32	6.15	5.07
Mg (mg/L)	<i>17.21</i>	23.48	43.54	30.29
Ca (mg/L)	<i>89.37</i>	<i>80.38</i>	<i>83.58</i>	111.08
TN (mg/L)	<i>1.53</i>	<i>1.68</i>	<i>2.23</i>	0.95
NPOC (mg/L)	<i>2.54</i>	<i>2.87</i>	7.78	5.94
δ ₁₈ O	<i>-4.88</i>	<i>-3.83</i>	<i>-4.94</i>	<i>-5.26</i>
δ ₂ H	<i>-30.41</i>	<i>-28.35</i>	<i>-29.92</i>	<i>-35.06</i>
Excess CO ₂	5.71	<i>3.97</i>	7.63	<i>5.05</i>

Average diel results compared to groundwater

Field measurements and geochemical analyses demonstrate that groundwater is distinct from stream chemistry at all diel sampling sites. Stable isotopes of water (δ₁₈O and δD) were generally lower for groundwater samples than corresponding stream samples. Samples from Vermillion Creek were an exception, as stream and groundwater isotopic ratios were similar (Figure 5). Mill and Vermillion signatures varied over the course of the day compared to the other sites, as seen by the deviation of samples from the GMWL at those two sites compared to the clustering of Chapman and Mulberry Creek samples. Groundwater temperature, pH, DO and potassium concentrations were lower than the 24-hour average for the corresponding stream measurements at each site (Figure 6; temperature and K not shown). Conductivity, chloride, alkalinity, sodium and calcium concentrations were typically higher in groundwater than stream samples, with Mulberry Creek as an exception. Bromide was also slightly higher in groundwater

than stream samples, however concentrations did not exceed 0.5 mg/L for any sample (not shown).

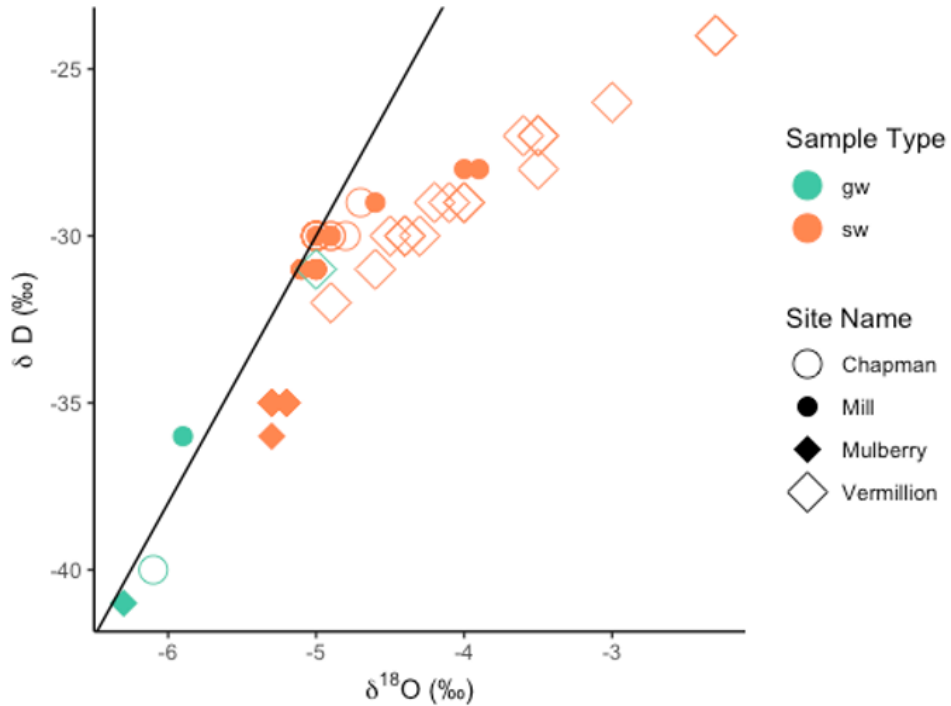


Figure 5 Stable isotopes of water plotted against the GWML. The color of the scatter plot markers indicates whether the sample was stream water (sw) or groundwater (gw) and the shape corresponds to the site.

In contrast, nutrient concentrations varied considerably with no consistent differences between stream and groundwater across the sites (Figure 6). At Chapman Creek, groundwater nitrate concentrations were lower than streamwater concentrations. Stream and groundwater nitrate concentrations were similar at Mulberry Creek, with groundwater concentrations slightly higher. Mill Creek and Vermillion Creek had groundwater nitrate concentrations well above stream concentrations. NPOC was typically lower in groundwater than streams at all sites except Mill Creek, where concentrations were similar.

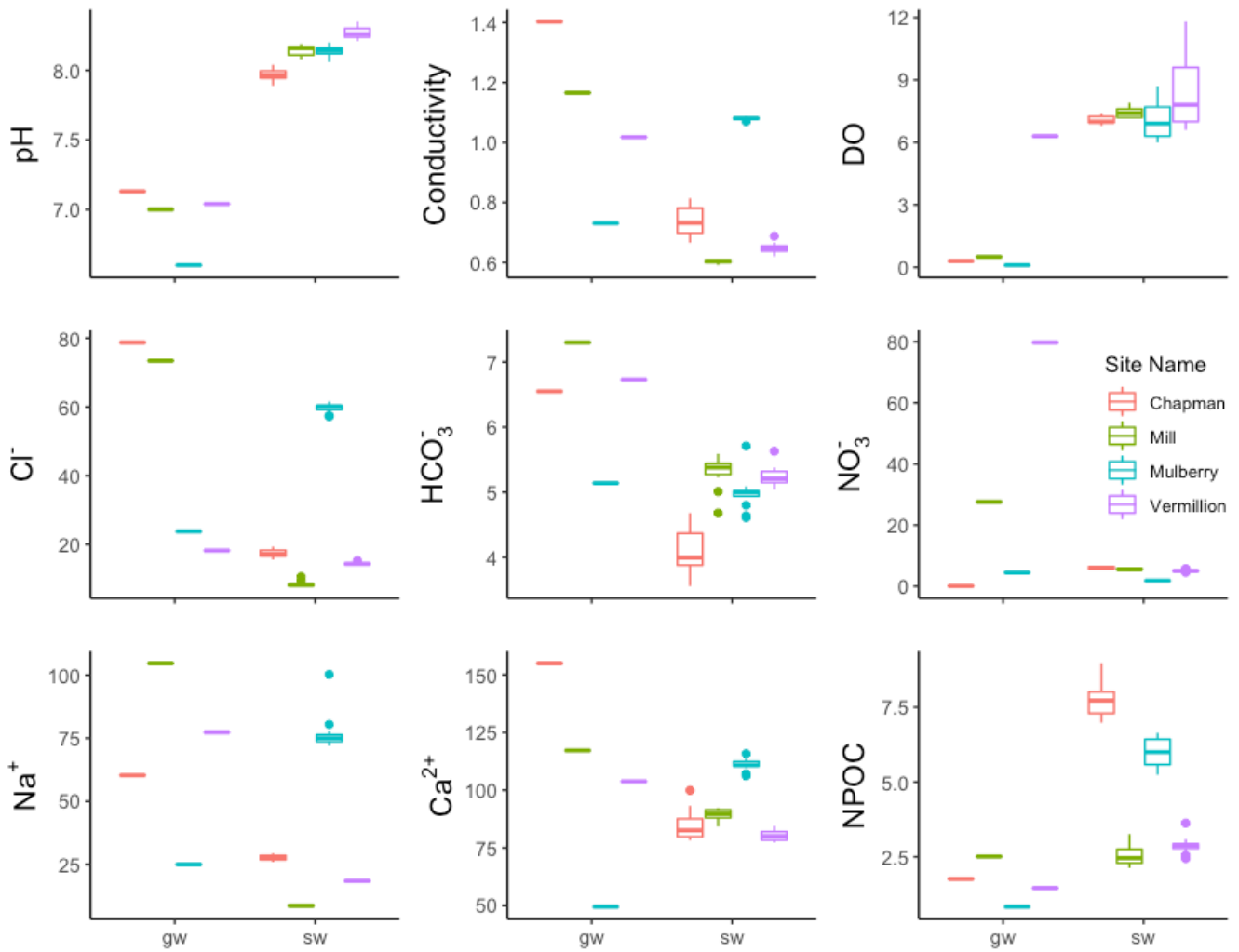


Figure 6 Variation in groundwater (gw) and stream water (sw) concentrations of a) pH, b) conductivity, c) DO, d) Cl⁻, e) alkalinity, f) nitrate, g) Na, h) Ca, i) NPOC. The color corresponds with site location.

Chapter 4 - Discussion

This study investigated how groundwater discharge varies across Kansas precipitation gradient and its impact on stream biogeochemistry. Results show that runoff and baseflow increase and BFI tends to decrease as the annual precipitation gets higher. Stream composition varies considerably, with many parameters demonstrating a decreasing trend with increasing precipitation. Below, we further discuss how these patterns relate to hydrogeology, annual precipitation and the land use of the study area.

Variability of groundwater discharge

Our analysis of hydrograph separation results reveals significant and unexpected relationships between streamflow components, groundwater discharge and precipitation. Baseflow and runoff both increase significantly ($P < 0.05$) with increasing precipitation (Figure 2, Table 24). We expected the contribution of groundwater to streamflow to also increase with precipitation. However, the calculated BFI values decrease significantly with increasing precipitation (Figure 2; $\rho = -0.44$, $P < 0.05$).

We interpret that these results reflect the influence of infiltration on the contribution of groundwater to streams. During precipitation events, some portion of the water infiltrates the surface, percolates downward, and ultimately recharges the underlying saturated zone. Thus, the amount of precipitation and permeability of the surface are controls on the absolute amount of groundwater discharge to streams (Price, 2011). However, runoff also increases with precipitation. If runoff increases more rapidly than recharge, then the relative contribution of groundwater to streamflow would decrease with precipitation, as we observed.

The rate of infiltration, and thus recharge, can be limited by variations in permeability of watershed surfaces, further explaining the decreasing trend in BFI across Kansas. Such variations can result from shifts in surficial and underlying geology. For example, western streams located on unconsolidated coarse sand and gravel deposits, sandstones and chinks. These deposits are associated with higher rates of groundwater transmission and can have hydraulic conductivity values (K) of $10^2 - 10^3$, 3.1 and 30 m/day respectively (de Marsily, 1986). As a result, these streams tend to have high amounts of groundwater discharge ($BFI > 0.40$).

The amount of clay in soils can also explain the discrepancies in proportion of baseflow and runoff trends eastward. High clay content in soils is associated with lower permeability and hydraulic conductivity (1-5 m/day) (de Marsily, 1986), resulting in limited infiltration and recharge (Hillel, 1982; Price,

2011; Goodman & Quigley, 2015). Although we do not observe a relationship between clay content and groundwater discharge explicitly ($\rho = -0.21$, $P = 0.29$), both parameters show significant variation across the precipitation gradient. Figure 7 demonstrates this relationship, as clay content of soils increases with precipitation (Table 20; $\rho = 0.46$, P

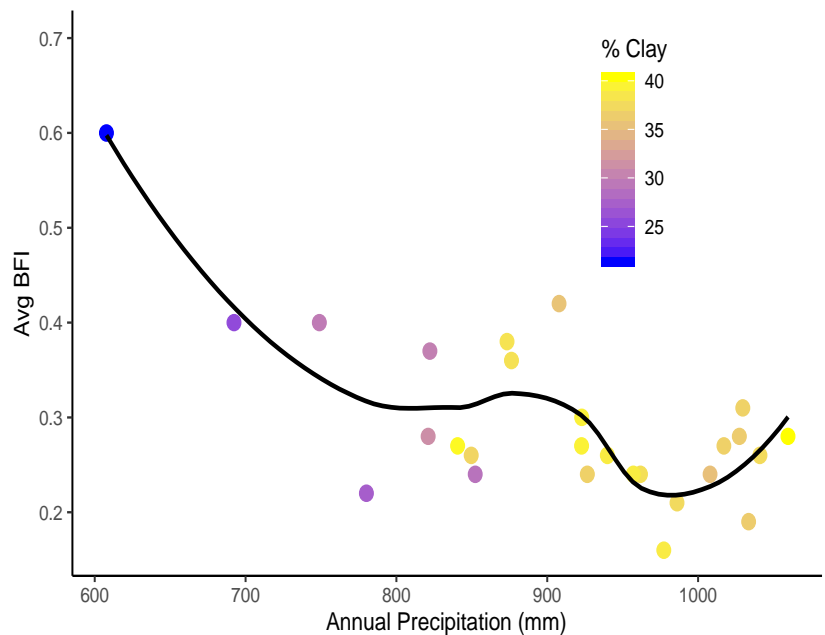


Figure 7 Average stream BFI decreases with increased precipitation (black trend line). The color of the points corresponds with watershed clay content. Higher clay content is yellow and lower clay content is purple to blue.

< 0.05) and proportion of baseflow decreases (Table 20; $\rho = -0.44$, $P < 0.05$).

Biogeochemical impact of groundwater discharge

The other aim of our study has been to identify whether differences in the contribution of groundwater discharge to streamflow (estimated by BFI) leaves a distinguishable fingerprint on stream chemistry. We hypothesize that the BFI, which is averaged over 15 years of streamflow records, can leave a sustained impact on stream chemistry by increasing the flux of solutes to streams and reducing the hyporheic zone. As precipitation infiltrates the lands surface to recharge groundwater, it interacts with soils that contain CO₂ with partial pressures that are 10-100X atmospheric levels (Macpherson, 2009). As a result, increases in groundwater concentrations of dissolved CO₂ can acidify the water which reacts with minerals, increasing the solute concentrations and pH of the water with distance and time (Jones et al., 2003). Therefore, streams receiving greater proportions of groundwater discharge may have higher concentrations of mineral weathering products, including carbonate alkalinity, alkali and alkali Earth metals, and silica (Dedzo et al., 2017). Moreover, anoxic conditions are common in aquifers because groundwater is isolated from the surface. Anoxic conditions can further be created through sequential redox reactions that are stimulated with groundwater mixing in streams (Triska et al., 1993; Rivett et al., 2008; Bethke et al., 2011). As a result, streams that receive greater inputs of groundwater may often have more reduced hyporheic zones, increased nutrient attenuation and overall water quality (Triska et al., 1993).

Results of our grab sampling efforts are consistent with aspects of this conceptual model. We observe that stream alkalinity concentrations increase with groundwater discharge from east to west ($\rho = 0.52$, $p < 0.005$). There is also a general transition from NaCl to Ca-HCO₃ water types eastward that reflects shifts in underlying geology, demonstrating that geogenic solutes are

being transported to streams (Figure 8). Total dissolved solids (TDS) follows this trend.

Groundwater is known to have increased concentrations of chemical weathering products such as alkalinity, major ions and TDS (Dedzo, 2017), and our results indicate these products could be transported to streams as a result of increased groundwater discharge.

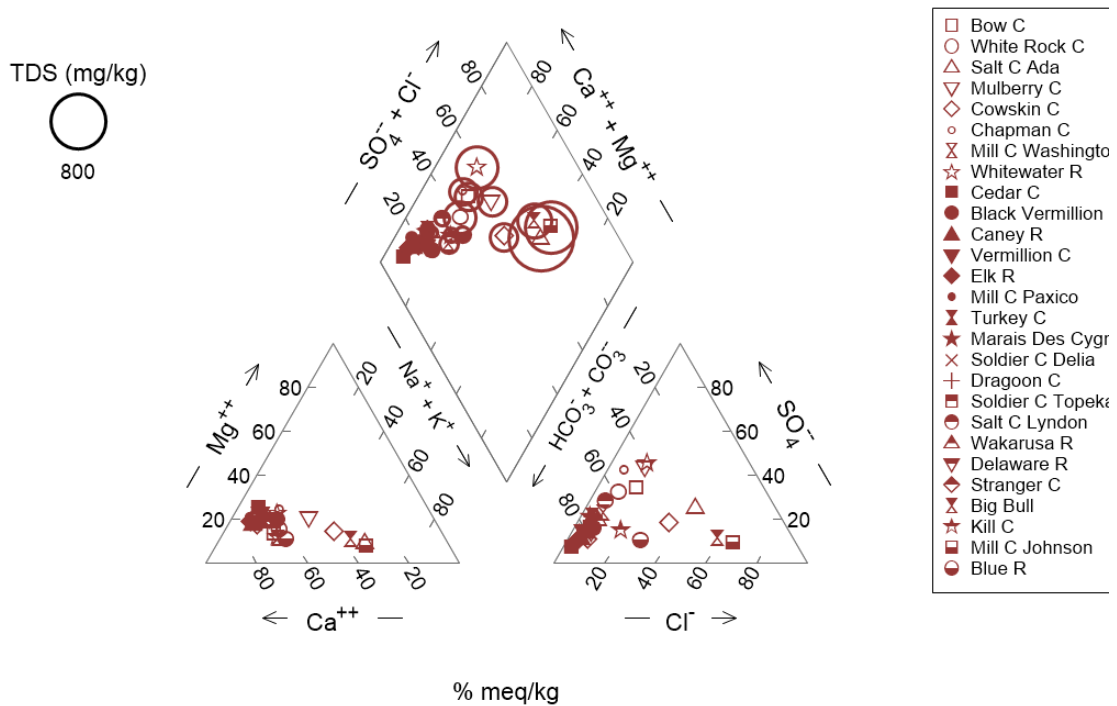


Figure 8 Piper diagram demonstrates that water type/major ion chemistry changes from the western sites to eastern sites. The circles around each site indicates TDS. The sites are listed from furthest west at the top (Bow Creek) to the furthest east at the bottom (Blue River).

Although we do not see many significant relationships between BFI and chemical results, we do observe numerous significant relationships with the clay content of watershed soils that can further demonstrate the clay as limiting factor in groundwater discharge to streams (Figure 9). Specifically, we observe that increases in clay content coincide with decreased stream concentrations for solutes that are associated with groundwater contribution Br, Li and B (Davis et al., 1998) and excess carbon dioxide ($P < 0.05$). Clay soils are known to have low hydraulic conductivity (1-5 m/day) that limits groundwater flow (de Marsily, 1986), explaining the lower concentrations of conservative tracers and dissolved CO_2 in streams.

Additionally, we observe lower concentrations of cations and metals (Na, K, Ca, Cd, Mo, As, Co, Ni) that may reflect increased sorption along flow paths

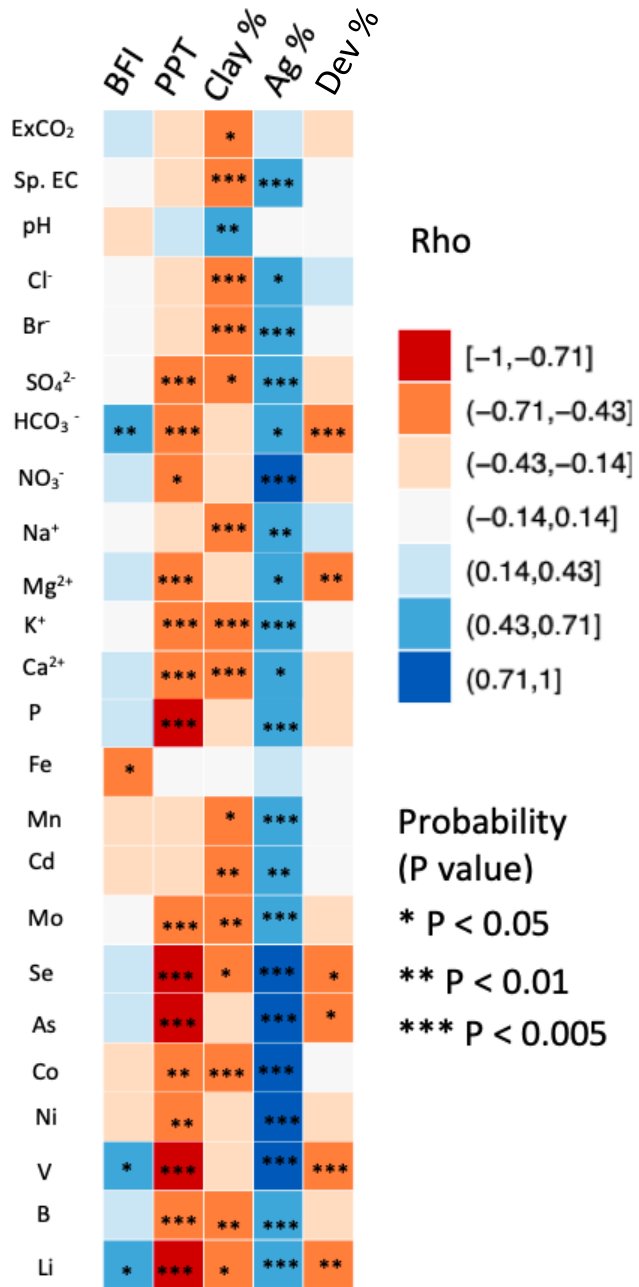


Figure 9 Correlation matrix comparing stream and watershed characteristics (BFI, annual precipitation, watershed clay content and the percent agriculture or developed). Color indicates correlation (rho) and asterisks indicate statistically significant relationships.

due to changes in soil texture (clay content) and mineralogy across the study area. Iron and organic carbon-rich soils have increased affinity for absorption of such elements, and recent findings indicate that organic carbon and ferric iron levels in soil increase across the precipitation gradient (Wang & Li, 2011; Ugwu & Igbokwe, 2019; Koenigsberger, in prep).

The results of our diel sampling further demonstrate that evidence of groundwater discharge can be observed in stream biogeochemistry. For example, creeks that have higher calculated BFI values show evidence of potential mixing of groundwater (Figure 10). More specifically, nitrate concentrations of groundwater at Mill Creek were higher (80 mg/L) than in streams and could potentially provide nitrate to streams. As streamflow increases, or as the proportion of baseflow from total streamflow decreases, the concentration of nitrate in those streams

decrease as well. In contrast, Mulberry Creek had the lowest BFI (0.22) and demonstrated inconsistent variations in stream nitrate chemistry.

In general, however, our diel results indicate that variations in stream chemistry is due to changes in diel (temperature/light) cycles as well as hydrology (BFI and discharge) at each site.

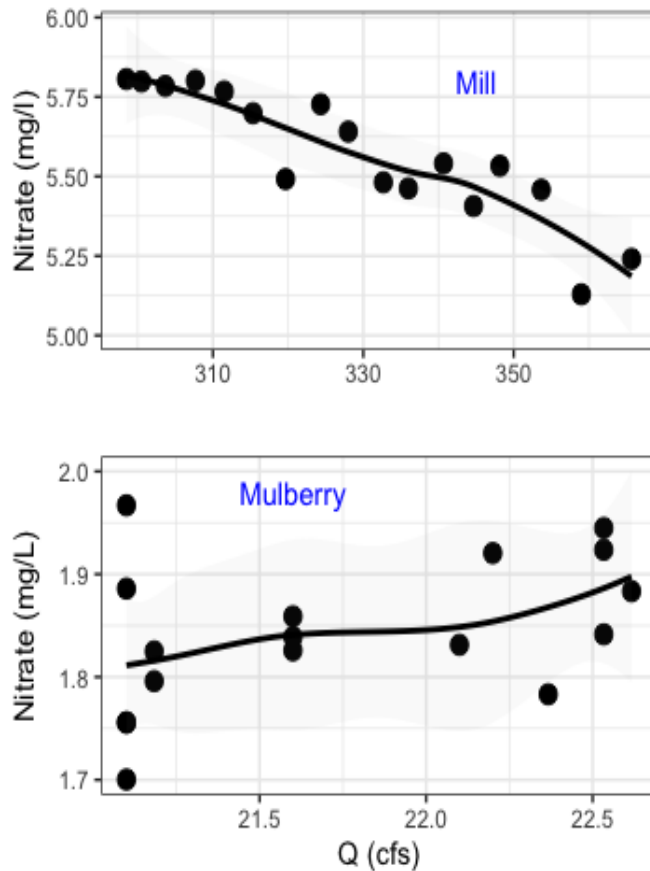


Figure 10 Concentration discharge graphs for stream with high BFI value Mill Creek (0.42) compared to lower BFI value stream Mulberry Creek (0.22).

More specifically, the extent of decrease in discharge over the sampling period appears to influence the magnitude of variation for parameters such as temperature, DO, pH, calcite saturation and excess carbon dioxide. For example, discharge at Mulberry and Vermillion Creek decreased by less than 5 cfs over the study period and show variability in concentrations that is typical of diel cycles (peaks occur during the day or night). In contrast, discharge at Mill and Chapman decreased by around 70 and 20 cfs respectively, and tend to have muted, less evident diel cycles. Full diel results can be found in Appendix C - Diel Sampling Results and observed in Appendix J - Extra Figures.

Additionally, our diel results suggest that the impact of diel variation on stream chemistry in our grab sampling is likely minimal. We carried out diel sampling during the summer and grab sampling in the winter. The variability of parameters from site to site was much larger than the diel variations we observed at each site, even during summer months when variations in temperature and discharge were more variable.

Role of land use on groundwater discharge and stream chemistry

Our results demonstrate that land use, both amount of development and agriculture in a watershed, influences streamflow components and the proportion of groundwater discharge to streams (Figure 11). More specifically, we observe that developed watersheds have higher runoff ($\rho = 0.59$, $p < 0.002$) and proportions of baseflow ($\rho = -0.54$, $P < 0.005$). These relationships

could be explained by the increase in impervious surfaces that, similar to clay, that allow for increased rates of runoff that limits recharge. Conversely, watersheds with higher agricultural percent have lower baseflow (rho = -0.77, $p < 0.0001$). Groundwater withdraw due to irrigation has been observed to lower groundwater levels and reduce groundwater discharge to streamflow, which could explain the negative relationship we observe

between agriculture and baseflow (Barlow & Leake, 2012; Juracek & Eng, 2017). However, further investigation of individual watershed management and practices is required to determine the cause of these observed relationships.

The impact of land use on stream chemistry is also evident from the results of our grab sampling approach. Of the 24 stream chemistry parameters we measured (Figure 9), 21 of the parameters demonstrate significant positive relationships with agriculture ($P < 0.05$). Although the amount of development in watersheds does not demonstrate many significant relationships with chemistry parameters, we do see streams that were consistently outliers were in more developed/urbanized watersheds (Cowskin Creek in Wichita, Mill Creek at Johnson and Big Bull Creek in Kansas City area). Additionally, Salt Creek at Ada was consistently an outlier and although it is not in a highly developed watershed, it is located near the Ottawa City landfill (2

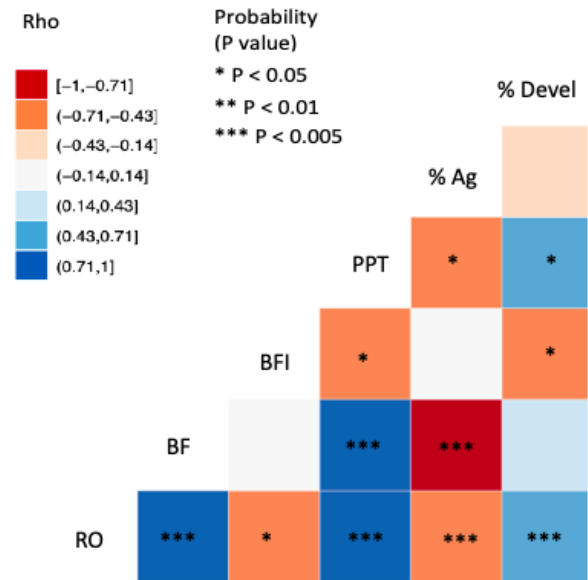


Figure 11 Correlation matrix comparing streamflow components (RO, BF, BFI) to watershed characteristics (annual precipitation, and the percent agriculture or developed). Color indicates correlation (rho) and asterisks indicate statistically significant relationships.

miles). Landfills are known to contain a wide variety of chemicals that can contaminate water resources (Jones-Lee & Lee, 1993).

The superimposed relationship between precipitation and land use should be addressed in order to draw sound conclusions from our results (Figure 11). For example, more developed watersheds tend to be in areas of higher annual rainfall ($\rho = 0.51$, $p < 0.01$), which could also explain high proportion of runoff in eastern streams. The reality is that the high runoff component of eastern streams is likely due to the combination of both precipitation and land use gradients across Kansas. Similarly, watersheds with increased agriculture tend to receive less precipitation annually ($\rho = -0.63$, $p < 0.005$), which could also explain the negative relationship between baseflow and the amount of agriculture. These results suggest that the influence of precipitation and land use on water quality are superimposed, which is important to take into consideration for future management of water resources.

Limitations

There are important limitations to our approaches that should be understood when interpreting the results of these analyses (Eckhardt, 2008; Barlow et al., 2015). The results of the hydrograph separation method are estimates, with true values of BFI often unknown, and studies to validate the results using chemical tracers are geographically limited (Eckhardt, 2008). Comparing the results for the six different methods is used to ensure accuracy (Barlow et al., 2015) and for our study such comparison suggests that the results are consistent across all sites (Figure 2). However, the use of hydrograph separations to determine baseflow conditions is widely used and useful metric for understanding relationships between groundwater discharge and watershed characteristics (Tesoriero et al., 2009; Price, 2011).

Limitations of our sampling approaches are important to address. The grab sampling approach allowed us to study a large spatial scale; however, we lack temporal data to account for variability of stream chemistry. Diel allows us to capture an aspect of temporal variation. However due to the nature of the 24-hour sampling, our spatial scale is limited. We utilized both approaches to account for the inherent disadvantage each method presents. Furthermore, the watershed characteristics to which we compare are hydrograph and geochemical results derived from national, open source geospatial data that uses modeled or extrapolated site-specific measurements to determine environmental features and anthropogenic influences of watersheds (USGS, 2016). Nevertheless, our sampling approaches and use of available watershed data allow for effective and extensive analysis of the influence of groundwater discharge on stream biogeochemistry.

Although we do observe strong and significant relationships, due to the nature of our study we were unable to determine the cause of groundwater discharge and stream chemistry trends or the extent that precipitation and/or land use influenced them. Regardless, our results add to the growing knowledge on the importance of groundwater discharge and that precipitation and land use often demonstrate complex relationships that convolute its effects on water quality and increases the need for further investigation (Price, 2011; Zipper et al., 2018; Sebastian et al., 2019).

Chapter 5 - Conclusion

We examined the variation of groundwater discharge across a portion of the Kansas precipitation gradient. Our results indicate that runoff and baseflow increase with annual precipitation eastward across Kansas. However, runoff and baseflow components of streamflow do not increase at the same rate. As a result, the proportion of groundwater discharge is lower in watersheds that receive more annual precipitation. This likely occurs due to the permeability of watershed surfaces negatively influencing rates of baseflow recharge. These differences are a result of both natural (shifts in soil clay content and lithology) as well as anthropogenic alteration of watershed surfaces.

We also sought to understand the implications of the variability of groundwater discharge on stream biogeochemistry. Our results show that stream biogeochemistry varies across the study area relative to changes in watershed hydrogeology and land use. Alkalinity has a significant relationship with groundwater discharge, however most chemical parameters have strong and significant relationships with clay content, suggesting that variations in clay content of watershed soils could serve as a potential limiting factor in nutrient and trace element loading to streams. Major ions chemistry is generally reflective of dominant watershed geology (water type shifts from NaCl to Ca-HCO₃ eastward), but also appears to be influenced by land cover (both percent agriculture and developed). Further highlighting the importance of land use on stream biogeochemistry, nutrients (nitrate/nitrogen and organic carbon), and trace elements are also strongly correlated with the percent of agriculture within watersheds.

Our study provides evidence that hydrogeology, precipitation and land use collectively influence stream components and biogeochemistry which has implications on overall water quality. Although we are unable to determine the direct cause of variability in groundwater

discharge and stream chemistry trends, our results add to the understanding of terrestrial and aquatic connectivity and emphasize the need to answer questions that remain regarding how future climate and anthropogenic changes will affect the quality of water resources.

References

- Barlow, P.M., Cunningham, W.L., Zhai, Tong, and Gray, M. (2015). U.S. Geological Survey Groundwater Toolbox, a graphical and mapping interface for analysis of hydrologic data (version 1.0)—User guide for estimation of base flow, runoff, and groundwater recharge from streamflow data: U.S. Geological Survey Techniques and Methods, book 3, chap. B10, 27 p., <http://dx.doi.org/10.3133/tm3B10>.
- Barlow, P.M., Cunningham, W.L., Zhai, Tong, and Gray, M. (2017) U.S. Geological Survey Groundwater Toolbox version 1.3.1, a graphical and mapping interface for analysis of hydrologic data: U.S. Geological Survey Software Release, 26 May 2017, <http://dx.doi.org/10.5066/F7R78C9G>
- Barlow, P.M., and Leake, S.A. (2012). Streamflow depletion by wells—Understanding and managing the effects of groundwater pumping on streamflow: U.S. Geological Survey Circular 1376, 84 p.
- Berrow, M., and L. Ure. (1986). "Trace Element Distribution and Mobilization in Scottish Soils with Particular Reference to Cobalt, Copper and Molybdenum." *Environmental Geochemistry and Health* 8.1 (1986): 19-24.
- Bethke, C. M. (2010). *Geochemical and Biogeochemical Reaction Modeling*. Cambridge University Press.
- Bethke, C. M., Sanford, R. A., Kirk, M. F., Jin, Q., & Flynn, T. M. (2011). The thermodynamic ladder in geomicrobiology. *American Journal of Science*, 311(3), 183–210.
- Boano, F., Harvey, J. W., Marion, A., Packman, A. I., Revelli, R., Ridolfi, L., & Wörman, A. (2014). Hyporheic flow and transport processes: Mechanisms, models, and biogeochemical implications. *Reviews of Geophysics*, 52(4), 603–679.
- Cavicchioli, R., Ripple, W.J., Timmis, K.N. et al. (2019). Scientists’ warning to humanity: microorganisms and climate change. *Nat Rev Microbiol* 17, 569–586.
- Clow, D. W., & Drever, J. I. (1996). Weathering rates as a function of flow through an alpine soil. *Chemical Geology*, 132(1–4), 131–141.
- Davis, S. N., Whittemore, D. O., & Fabryka-Martin, J. (1998). Uses of Chloride/Bromide Ratios in Studies of Potable Water. *Groundwater*, 36(2), 338–350.
- De Marsily, G. (1986). *Quantitative Hydrogeology*. Academic Press, Paris.
- Dedzo, M. G., Tsozué, D., Mimba, M. E., Teddy, F., Nembungwe, R. M., & Linida, S. (2017). Importance of Rocks and Their Weathering Products on Groundwater Quality in Central-East Cameroon. *Hydrology*, 4(2), 23.

- Diaz, R.J., Nestlerode, J., Diaz, M.L. (2004). A global perspective on the effects of eutrophication and hypoxia on aquatic biota. In: Rupp, G.L., White, M.D. (Eds.), Proc. 7th International Symposium Fish Physiology, Toxicology and Water Quality, Tallinn, Estonia. 600/R-04/049. US Environmental Protection Agency, Ecosystems Research Division, Athens, Georgia.
- Dodds, W. K., Gido, K., Whiles, M. R., Daniels, M. D., & Grudzinski, B. P. (2015). The Stream Biome Gradient Concept: factors controlling lotic systems across broad biogeographic scales. *Freshwater Science*, 34(1), 1–19.
- Domagalski, J.L., & Johnson, H.M. (2011). Subsurface transport of orthophosphate in five agricultural watersheds, USA. *Journal of Hydrology* 409: 157-171
- Domagalski, J. L., Ator, S., Coupe, R., McCarthy, K., Lampe, D., Sandstrom, M., & Baker, N. (2008). Comparative Study of Transport Processes of Nitrogen, Phosphorus, and Herbicides to Streams in Five Agricultural Basins, USA. *Journal of Environmental Quality*, 37(3), 1158–1169.
- Dubrovsky, N. M., & Geological Survey (U.S.) (Eds.). (2010). Nutrients in the nation’s streams and groundwater, 1992-2004. U.S. Geological Survey.
- Eckhardt, K. (2008). A comparison of baseflow indices, which were calculated with seven different baseflow separation methods. *Journal of Hydrology*, 352(1–2), 168–173.
- Foster, G.M., Graham, J.L., and King, L.R., 2019, Spatial and temporal variability of harmful algal blooms in Milford Lake, Kansas, May through November 2016: U.S. Geological Survey Scientific Investigations Report 2018–5166, 36 p.
- Falcone, J. A. (2011). GAGES-II: Geospatial Attributes of Gages for Evaluating Streamflow (Report). Reston, VA. <https://doi.org/10.3133/70046617>
- Frei RJ, Abbott BW, Dupas R, Gu S, Gruau G, Thomas Z, Kolbe T, Aquilina L, Labasque T, Laverman A, Fovet O, Moatar F and Pinay G (2020). Predicting Nutrient Incontinence in the Anthropocene at Watershed Scales. *Front. Environ. Sci.* 7:200.
- Goodman J. A., & Quigley M. (2015). Active Hydromodification Control. International Low Impact Development Conference 2015, 1–10.
- Hartmann, A., Goldscheider, N., Wagener, T., Lange, J., & Weiler, M. (2014). Karst water resources in a changing world: Review of hydrological modeling approaches. *Reviews of Geophysics*, 52(3), 218–242. <https://doi.org/10.1002/2013RG000443>
- Harvey, J. W., Böhlke, J. K., Voytek, M. A., Scott, D., & Tobias, C. R. (2013). Hyporheic zone denitrification: Controls on effective reaction depth and contribution to whole-stream mass balance: Scaling hyporheic flow controls on stream denitrification. *Water Resources Research*, 49(10), 6298–6316.

- Hillel, D. (1982). Introduction to environmental soil physics. Academic Press. ISBN 9780080918693.
- Indraratne., S. P., Kumaragamage, D. (2017). Flooding-induced mobilization of potentially toxic trace elements from uncontaminated, calcareous agricultural soils. *Canadian Journal of Soil Science*, 2018, 98:103-113
- Jasechko, S. (2019). Global isotope hydrogeology-Review. *Reviews of Geophysics*, 57, 835-965
- Jasechko, S., Kirchner, J.W., Welker, J.M, McDonnell, J.J. (2016). Substantial proportion of global streamflow less than three months old
- Jones, J., Grows, I., Arnold, A., McCall, S., Bowes, M. (2015). The effects of increased flow and fine sediment on hyporheic invertebrates and nutrients in stream mesocosms. *Freshwater Biology*: 1-36
- Jones, J. B., Stanley, E. H., & Mulholland, P. J. (2003). Long-term decline in carbon dioxide supersaturation in rivers across the contiguous United States: DECLINE IN RIVERINE CARBON DIOXIDE. *Geophysical Research Letters*, 30(10).
- Jones-Lee, A. and Lee, G. F. (1993). 'Groundwater Pollution by Municipal Landfills: Leachate Composition, Detection and Water Quality Significance,' Proc. Sardinia '93 IV International Landfill Symposium, Sardinia, Italy, pp. 1093-1103.
- Juracek, K.E., and Eng, Ken. (2017). Streamflow alteration at selected sites in Kansas: U.S. Geological Survey Scientific Investigations Report 2017–5046, 75 p.
- Kansas Geological Survey (KGS). (2008). Surficial geology of Kansas: Kansas Geologic Survey, Map M-118, scale 1:500,000.
- Koenigsberger, in prep
- Lin, X., Harrington, J., Ciampitti, I., Gowda, P., Brown, D., & Kisekka, I. (2017). Kansas Trends and Changes in Temperature, Precipitation, Drought, and Frost-Free Days from the 1890s to 2015. *Journal of Contemporary Water Research & Education*, 162(1), 18–30.
- Loecke, T.D., Burgin, A.J., Riveros-Iregui, D.A. et al. *Biogeochemistry* (2017) 133: 7.
- Lui, Y., Zarfl, C., Basu, N. B., Schwientek, M., Cirpka, O. A. (2018). Contributions of catchment and in stream processes to suspended sediment transport in a dominantly groundwater-fed catchment. *Hydrology and Earth System Sciences*, 22: 3903-3921
- Macpherson, G. (2009). CO₂ distribution in groundwater and the impact of groundwater extraction on the global C cycle. *Chemical Geology* 264. 328-336.
- Macpherson, G., Sullivan, P., (2019). Watershed-scale chemical weathering in a merokarst

- terrain, northeastern Kansas, USA. Evolution of Carbonate and Karst Critical Zones. *Chemical Geology*, (527).
- Macfarlane, P. A, Misgna, G. M., Buddemeier, R. W., (2000). Atlas of Kansas High Plains Aquifer: Preliminary Analysis of Potential Ground-water Supplies. *Kansas Geological Survey Educational Series 14*.
- Mulholland, P. J., Helton, A. M., Poole, G. C., Hall, R. O., Hamilton, S. K., Peterson, B. J., ... Thomas, S. M. (2008). Stream denitrification across biomes and its response to anthropogenic nitrate loading. *Nature*, 452(7184), 202–205.
- Nimick, D. A., Gammons, C. H., & Parker, S. R. (2011). Diel biogeochemical processes and their effect on the aqueous chemistry of streams: A review. *Chemical Geology*, 283(1–2), 3–17.
- Park, J.-H., Duan, L., Kim, B., Mitchell, M. J., & Shibata, H. (2010). Potential effects of climate change and variability on watershed biogeochemical processes and water quality in Northeast Asia. *Environment International*, 36(2), 212–225.
- Peralta-Maraver, I., Reiss, J., & Robertson, A. L. (2018). Interplay of hydrology, community ecology and pollutant attenuation in the hyporheic zone. *Science of The Total Environment*, 610–611, 267–275.
- Price, K. (2011). Effects of watershed topography, soils, land use, and climate on baseflow hydrology in humid regions: A review. *Progress in Physical Geography: Earth and Environment*, 35(4), 465–492.
- PRISM Climate Group, Oregon State University, <http://prism.oregonstate.edu>, created January 2020.
- QGIS Development Team, (2017). QGIS Geographic Information System. Open Source Geospatial Foundation Project. <http://qgis.osgeo.org>
- RStudio Team (2019). RStudio: Integrated Development for R. RStudio, Inc., Boston, MA URL <http://www.rstudio.com/>
- Rahmani, V., Hutchinson, S. L., Jr, J. A. H., Hutchinson, J. M. S., & Anandhi, A. (2015). Analysis of temporal and spatial distribution and change-points for annual precipitation in Kansas, USA. *International Journal of Climatology*, 35(13), 3879–3887. <https://doi.org/10.1002/joc.4252>
- Rawitch, M., Macpherson, G.L. & Brookfield (2019). Exploring methods of measuring CO2 degassing in headwater streams. *Sustainable Water Resources Management*.
- Richard, A., (2018). Variation in groundwater geochemistry and microbial communities in the High Plains aquifer system, south-central Kansas.

- Rivett, M. O., Buss, S. R., Morgan, P., Smith, J. W. N., & Bemment, C. D. (2008). Nitrate attenuation in groundwater: A review of biogeochemical controlling processes. *Water Research*, 42(16), 4215–4232.
- Sander, R. (1999). Compilation of Henry's Law Constants for Inorganic and Organic Species of Potential Importance in Environmental Chemistry. Air Chemistry Department Max-Planck Institute of Chemistry
- Schade, J. D., Bailio, J., & McDowell, W. H. (2016). Greenhouse gas flux from headwater streams in New Hampshire, USA: Patterns and drivers: Greenhouse gas flux from headwater streams. *Limnology and Oceanography*, 61(S1), S165–S174.
- Seager, R., Lis, N., Feldman, J., Ting, M., Williams, A. P., Nakamura, J., Liu, H., Henderson, N. (2017). Whither the 100th Meridian? The Once and Future Physical and Human Geography of America's Arid-Humid Divide. Part 1: The Story So Far. *Earth Interactions*, 22: 1-22
- Stegen, J. C., Fredrickson, J. K., Wilkins, M. J., Konopka, A. E., Nelson, W. C., Arntzen, E. V., Chrisler, W. B., Chu, R. K., Danczak, R. E., Fansler, S. J., Kennedy, D. W., Resch, C. T., & Tfaily, M. (2016). Groundwater–surface water mixing shifts ecological assembly processes and stimulates organic carbon turnover. *Nature Communications*, 7(1), 11237.
- Stoeser, D., Green, G., Morath, J., Heran, W., Wilson, A., Moore, D., Van Gosen, B. (2005). Preliminary Integrated Geologic Map Databases for the United States Central States: Montana, Wyoming, Colorado, New Mexico, Kansas, Oklahoma, Texas, Missouri, Arkansas, and Louisiana, - The State of Kansas. Map. U.S. Geological Survey Open-File Report 2005-1351, Denver, CO. Using GIS software: QGIS.
- Stookey LL (1970) Ferrozine - a new spectrophotometric reagent for iron. *Analytical Chemistry*, 42, 779-781.
- Szramek, K., Walter, L.M. (2004). Impact of Carbonate Precipitation on Riverine Inorganic Carbon Mass Transport from a Mid-continent, Forested Watershed. *Aquatic Geochemistry* 10, 99–137.
- Tesoriero, A. J., Duff, J. H., Wolock, D. M., Spahr, N. E., & Almendinger, J. E. (2009). Identifying Pathways and Processes Affecting Nitrate and Orthophosphate Inputs to Streams in Agricultural Watersheds. *Journal of Environmental Quality*, 38(5), 1892–1900.
- Triska, F. J., Duff, J. H., & Avanzino, R. J. (1993). The role of water exchange between a stream channel and its hyporheic zone in nitrogen cycling at the terrestrial-aquatic interface. *Hydrobiologia* 251: 167-184, 18.
- Ugwu, I. M., & Igbokwe, O. A. (2019). Sorption of Heavy Metals on Clay Minerals and Oxides: A Review. *Advanced Sorption Process Applications*.

- U.S. Geological Survey, (2016). National Water Information System data available on the World Wide Web (USGS Water Data for the Nation).
- Vercruyse, K., Grabowski, R., Rickson, R.J., (2017). Suspended sediment transport dynamics in rivers: Multi-scale drivers of temporal variation. *Earth-Science Reviews*, 166: 38-52
- Wang XL, Li Y (2011). Measurement of Cu and Zn adsorption onto surficial sediment components: New evidence for less importance of clay minerals. *Journal of Hazardous Materials*. 2011;189(3):719-723.
- Winter, T. C. (2001). Ground water and surface water: the linkage tightens, but challenges remain. *Hydrological Processes*, 15(18), 3605–3606.
- Wondzell, S. M. (2011). The role of the hyporheic zone across stream networks. *Hydrological Processes*, 25(22), 3525–3532.
- Zeglin, L. H., Crenshaw, C. L., Dahm, C. N., Sheibley, R. W., & Takacs-Vesbach, C. D. (2019). Watershed hydrology and salinity, but not nutrient chemistry, are associated with arid-land stream microbial diversity. *Freshwater Science*, 38(1), 77–91.
- Zipper SC, MM Motew, EG Booth, X Chen, J Qiu, CJ Kucharik, SR Carpenter, SP Loheide II (2018). Continuous separation of land use and climate effects on the past and future water balance. *Journal of Hydrology*.

Appendix A - Hydrograph Separation Results

Table 3 Results of the Hydrograph Separation from USGS GW Toolbox. Results are normalized to drainage area (DA), thus units are inches/area. Streamflow components are baseflow (BF), runoff (RO) and baseflow index (BFI). This table hold results for Part and BFI standard (BFIStd).

Site	DA (mi ²)	Stream flow	BF Part	RO Part	BFI Part	BF BFIStd	RO BFIStd	BFI BFIStd
1. BOW C	341	0.62	0.35	0.27	0.64	0.3	0.33	0.55
2. WHITE ROCK C	227	1.22	0.46	0.76	0.42	0.38	0.84	0.35
3. SALT C (ADA)	406	1.71	0.72	0.99	0.45	0.47	1.24	0.32
4. MULBERRY C	261	1.79	0.37	1.43	0.25	0.26	1.54	0.18
5. COWSKIN C	86	4.94	0.93	4.01	0.26	0.56	4.38	0.18
6. CHAPMAN C	300	3.43	1.21	2.23	0.4	1	2.43	0.34
7. MILL C (WASH)	344	3.32	0.96	2.36	0.31	0.72	2.6	0.24
8. WHITEWATER R	426	6.99	1.53	5.46	0.29	1.11	5.88	0.23
9. CEDAR C (CEDAR POINT)	110	8.2	2.96	5.24	0.43	2.19	6.01	0.32
10. BLACK VERMILLION	410	4.72	1.3	3.42	0.3	0.88	3.84	0.22
11. CANEY R	445	9.2	3.39	5.81	0.41	1.74	7.45	0.2
12. VERMILLION C	243	4.59	1.68	2.91	0.4	1.2	3.38	0.29
13. ELK R	220	9.3	2.85	6.45	0.34	1.46	7.84	0.17
14. MILL C (PAXICO)	318	6.65	3.07	3.58	0.5	2.18	4.47	0.36
15. TURKEY C	276	4.52	1.42	3.1	0.32	1.03	3.5	0.22
16. MARAIS DES CYGNES R	177	6.58	1.69	4.89	0.27	1.04	5.54	0.17
17. SOLDIER C (DELIA)	149	6.67	1.89	4.78	0.34	1.32	5.35	0.24
18. DRAGOON C	114	7.1	1.6	5.5	0.24	0.95	6.16	0.14
19. SOLDIER C (TOPEKA)	290	6.5	1.76	4.74	0.31	1.26	5.23	0.22
20. SALT C (LYNDON)	97.8	7.73	1.23	6.5	0.17	0.7	7.03	0.1
21. WAKARUSA R	164	7	1.85	5.15	0.28	1.01	5.99	0.15
22. DELAWARE R (MUSCOTAH)	431	6.45	1.65	4.8	0.28	1.16	5.29	0.2
23. STRANGER C (TONGANOXIE)	406	8.12	2.07	6.05	0.28	1.37	6.75	0.19
24. BIG BULL C (EDGERTON)	28.7	10.06	1.57	8.48	0.17	0.83	9.23	0.09
25. KILL C (DESOTO)	53.4	9.15	2.67	6.49	0.32	1.61	7.54	0.2
26. MILL C (JOHNSON)	58.1	13.67	4.32	9.35	0.33	2.8	10.87	0.21
27. BLUE R (OVERLAND PARK)	65.8	11.46	3.44	8.03	0.32	1.89	9.57	0.17

Table 4 Results of the Hydrograph Separation from USGS GW Toolbox. Results are normalized to drainage area (DA), thus units are inches/area. Streamflow components are baseflow (BF), runoff (RO) and baseflow index (BFI). This table hold results for modified BFI (BFIMod) and all HySEP methods: HySEP Fixed, HySEP LocMin, HySEP Slide.

Site	BF BFIMod	RO BFIMod	BFI BFIMod	BF Fixed	RO Fixed	BFI Fixed	BF LocMin	RO LocMin	BFI LocMin	BF Slide	RO Slide	BFI Slide
1.	0.3	0.33	0.55	0.34	0.28	0.63	0.31	0.32	0.57	0.34	0.29	0.63
2.	0.38	0.84	0.34	0.48	0.74	0.44	0.43	0.8	0.39	0.48	0.74	0.44
3.	0.48	1.23	0.32	0.79	0.92	0.47	0.61	1.1	0.37	0.79	0.92	0.47
4.	0.25	1.54	0.18	0.36	1.44	0.24	0.3	1.49	0.21	0.36	1.44	0.24
5.	0.56	4.38	0.18	1.11	3.83	0.29	0.89	4.05	0.24	1.14	3.81	0.29
6.	1	2.43	0.34	1.13	2.3	0.38	1.08	2.35	0.37	1.15	2.29	0.38
7.	0.71	2.61	0.24	0.89	2.43	0.29	0.81	2.51	0.27	0.91	2.41	0.3
8.	1.1	5.89	0.23	1.63	5.35	0.3	1.4	5.59	0.27	1.59	5.4	0.29
9.	2.16	6.04	0.31	2.91	5.3	0.42	2.71	5.49	0.39	2.93	5.27	0.42
10	0.88	3.84	0.22	1.21	3.51	0.28	1.05	3.68	0.26	1.21	3.51	0.28
11	1.73	7.46	0.2	3.1	6.09	0.37	2.48	6.71	0.29	3.09	6.11	0.37
12	1.19	3.39	0.29	1.76	2.83	0.41	1.54	3.04	0.37	1.71	2.88	0.41
13	1.46	7.84	0.17	2.97	6.33	0.36	2.4	6.9	0.29	3.13	6.17	0.36
14	2.15	4.5	0.35	2.73	3.92	0.45	2.39	4.26	0.39	2.77	3.87	0.45
15	1.02	3.51	0.22	1.32	3.2	0.3	1.19	3.34	0.26	1.33	3.19	0.3
16	1.03	5.55	0.17	1.82	4.76	0.3	1.47	5.11	0.24	1.82	4.76	0.3
17	1.3	5.37	0.24	1.92	4.75	0.34	1.7	4.97	0.3	1.93	4.74	0.34
18	0.94	6.17	0.14	1.69	5.42	0.26	1.42	5.68	0.21	1.67	5.43	0.26
19	1.26	5.24	0.22	1.61	4.88	0.28	1.45	5.05	0.25	1.64	4.86	0.29
20	0.7	7.03	0.1	1.38	6.35	0.21	1.1	6.63	0.16	1.4	6.33	0.2
21	1	5.99	0.15	1.98	5.02	0.3	1.59	5.41	0.24	2	4.99	0.3
22	1.15	5.3	0.2	1.59	4.87	0.26	1.38	5.07	0.23	1.59	4.86	0.27
23	1.39	6.73	0.19	2.08	6.04	0.28	1.74	6.38	0.23	1.99	6.13	0.27
24	0.81	9.24	0.09	2.43	7.62	0.27	1.94	8.12	0.21	2.56	7.5	0.28
25	1.61	7.55	0.2	2.59	6.56	0.31	2.25	6.9	0.27	2.65	6.5	0.32
26	2.78	10.89	0.21	4.31	9.36	0.33	3.8	9.87	0.29	4.28	9.39	0.33
27	1.89	9.57	0.17	3.35	8.12	0.31	2.79	8.68	0.26	3.39	8.07	0.31

Table 5 Standard deviation between the six hydrograph separation analyses for each component (BF, RO, BFI). Streams with greatest standard deviation tend to occur in watersheds with higher annual precipitation values (in bold).

Site	BF	RO	BFI	Annual PPT
1.	0.023	0.027	0.043	607.74
2.	0.046	0.047	0.044	692.33
3.	0.146	0.146	0.072	748.91
4.	0.054	0.051	0.031	780.1
5.	0.256	0.253	0.050	852.27
6.	0.085	0.081	0.024	822.19
7.	0.104	0.104	0.030	821.08
8.	0.237	0.239	0.031	922.76
9.	0.373	0.372	0.053	873.33
10.	0.180	0.181	0.033	849.62
11.	0.724	0.721	0.091	1029.67
12.	0.257	0.252	0.057	876.28
13.	0.752	0.752	0.090	1059.66
14.	0.367	0.368	0.059	907.85
15.	0.167	0.172	0.043	840.59
16.	0.366	0.366	0.060	961.79
17.	0.296	0.296	0.049	922.88
18.	0.349	0.352	0.056	986.09
19.	0.208	0.207	0.038	939.9
20.	0.317	0.317	0.048	977.31
21.	0.463	0.462	0.071	957.06
22.	0.225	0.223	0.035	926.58
23.	0.329	0.329	0.043	1007.97
24.	0.761	0.760	0.084	1033.55
25.	0.504	0.504	0.057	1017.12
26.	0.743	0.743	0.059	1027.41
27.	0.737	0.734	0.070	1041.02

Appendix B - Grab Sampling Results

Table 6 Field measured data and major anions for grab sampling. Units are mg/L for all parameters except T (C), EC (mS), pH and alkalinity (meq/L).

Stream	Date	pH	DO	Temp	EC	F	Cl	Br	NO ₃	SO ₄	Alk
1.	2/24/20	8.22	12.7	6.75	0.95	0.397	59.659	0.218	4.272	177.736	5.38
2.	2/25/20	8.14	14.6	5.53	1.2	0.335	46.857	0.245	8.889	218.032	8.17
3.	2/3/20	6.92	11.6	4.4	2.17	0.268	324.253	0.314	3.675	256.171	6.55
4.	2/3/20	7.64	12.7	5.2	1.03	0.346	51.102	0.154	0.533	213.353	4.25
5.	2/10/20	9.46	20.3	5.55	0.965	0.245	136.138	0.221	3.79	92.337	4.76
6.	2/1/20	7.98	14.1	2.55	0.97	0.297	25.743	0.134	5.552	217.097	5.51
7.	2/19/20	8.26	12.5	2.6	0.88	0.272	27.951	0.15	7.455	103.035	6.46
8.	2/10/20	8.63	16.7	5.35	1.319	0.291	73.294	0.329	10.317	321.092	5.87
9.	2/10/20	8.9	17.5	5.5	0.545	0.305	6.542	0.042	0.189	20.097	5.11
10.	2/19/20	8.21	12.7	3.45	0.69	0.275	19.094	0.102	10.45	49.927	5.16
11.	2/16/20	8.27	13.3	4.9	0.525	0.223	9.608	0.06	0.158	26.827	4.25
12.	2/19/20	8.29	12.7	2.75	0.69	0.306	11.344	0.057	4.918	50.684	5.88
13.	2/16/20	8.24	12.7	3.3	0.52	0.211	8.579	0.058	0.871	26.242	4.57
14.	2/1/20	8.19	13.5	3.9	0.61	0.268	9.335	0.059	1.782	44.366	5.33
15.	2/19/20	8.28	13.3	3.15	0.675	0.325	10.625	0.083	8.846	63.666	4.62
16.	2/5/20	8.55	13	2.7	0.63	0.211	9.389	0.052	1.297	71.061	5.18
17.	2/1/20	8.42	13.8	3.1	0.62	0.278	12.182	0.067	2.878	47.67	5.19
18.	2/5/20	8.47	13.5	3.05	0.68	0.214	14.161	0.058	2.606	75.059	5.48
19.	2/1/20	8.27	13.6	4.25	0.6	0.233	14.096	0.065	3.462	48.826	4.91
20.	2/5/20	8.24	13.9	3.25	0.65	0.197	14.992	0.077	2.158	92.229	4.45
21.	2/5/20	8.33	13.1	2.55	0.575	0.202	17.025	0.063	1.614	59.872	4.56
22.	2/19/20	8.28	13.6	2.4	0.62	0.27	18.755	0.086	8.251	43.954	5.09
23.	2/17/20	8.22	12.9	2.4	0.62	0.234	18.528	0.077	5.449	31.345	5.04
24.	2/17/20	7.91	12.3	3.3	1.38	0.168	257.525	0.207	1.153	66.766	3.63
25.	2/17/20	8.54	17.4	5.1	0.69	0.25	46.19	0.085	3.259	50.238	4.56
26.	2/17/20	8.28	15.1	4.6	2.04	0.196	395.557	0.248	7.386	71.955	4.14
27.	2/17/20	8.2	18	4.5	0.78	0.192	77.241	0.098	0.905	35.721	4.54

Table 7 Major cations and nutrients data for grab sampling. Units are mg/L for all parameters except for Mn and Fe which are ppb.

Stream	Date	Na	Mg	K	Ca	Mn	Fe	P	NPOC	TN
1.	2/24/20	29	11.1	6	93.0	13	13	2	3.78	1.20
2.	2/25/20	41	16.3	6	113.8	347	10	1	4.62	2.20
3.	2/3/20	214	18.5	6	105.9	197	14	1	6.99	1.38
4.	2/3/20	50	18.6	3	72.3	292	26	0	3.66	0.29
5.	2/10/20	67	12.3	5	59.4	89	63	0	6.82	1.50
6.	2/1/20	25	20.2	3	81.7	275	37	1	5.95	1.86
7.	2/19/20	31	8.2	3	82.2	305	5	1	4.08	1.90
8.	2/10/20	35	26.0	3	114.1	111	30	0	4.85	2.61
9.	2/10/20	7	12.0	1	52.5	21	22	0	2.72	0.21
10.	2/19/20	18	11.0	2	56.8	191	77	1	5.11	2.66
11.	2/16/20	8	8.0	1	54.9	10	2	0	3.49	0.52
12.	2/19/20	10	12.8	2	63.0	81	39	0	3.56	1.32
13.	2/16/20	6	7.6	1	49.5	27	6	0	3.20	0.61
14.	2/1/20	6	10.1	1	58.4	27	4	0	2.55	0.56
15.	2/19/20	12	12.5	2	66.9	32	26	1	4.33	2.33
16.	2/5/20	10	10.1	2	56.2	49	46	0	5.12	0.71
17.	2/1/20	8	9.7	2	50.8	46	9	0	5.15	1.00
18.	2/5/20	11	10.6	1	60.1	79	74	0		
19.	2/1/20	11	9.0	2	49.7	71	9	0	4.93	1.12
20.	2/5/20	12	9.0	2	51.5	85	45	0		
21.	2/5/20	10	8.0	2	47.4	45	7	0		
22.	2/19/20	13	9.8	2	52.6	63	13	0		
23.	2/17/20	9	7.8	2	53.2	148	36	0		
24.	2/17/20	88	9.7	3	57.1	128	45	0		
25.	2/17/20	21	6.5	2	58.0	51	12	0		
26.	2/17/20	167	11.7	3	81.1	54	42	0		
27.	2/17/20	27	5.8	1	57.2	64	8	0		

Table 8 Trace element concentrations for grab sampling. Units for Li, B, Ni, Co, As, Se, Mo and Co are ppt. V, Cu and Zn are ppb.

Stream	Date	Li	B	V	Ni	Co	Cu	Zn	As	Se	Mo	Cd
1.	2/24/20	14585	32396	6	759	146	1	7	3779	6065	5071	27
2.	2/25/20	18826	37163	5	1430	537	1	8	3516	7972	5387	26
3.	2/3/20	39011	72652	5	1544	489	1	3	2721	1572	4352	25
4.	2/3/20	14367	40463	1	795	395	1	1	727	522	666	292
5.	2/10/20	6226	42963	3	1580	609	1	4	1439	630	2146	51
6.	2/1/20	10207	42670	2	1182	492	1	17	1374	1327	590	226
7.	2/19/20	8126	19578	2	952	605	2	108	1780	1897	2291	22
8.	2/10/20	11201	48481	2	969	308	4	5	1606	1249	1799	21
9.	2/10/20	2392	11600	1	169	96	1	1	656	217	1098	14
10.	2/19/20	4476	17904	2	1921	368	2	4	2450	1641	1178	36
11.	2/16/20	1480	12174	0	-150	69	0	7	310	159	177	7
12.	2/19/20	4349	17656	1	866	186	4	9	1056	1016	748	37
13.	2/16/20	1409	10049	0	-56	90	0	11	340	157	164	9
14.	2/1/20	2684	12204	1	-13	107	2	2	611	367	333	11
15.	2/19/20	7180	18856	2	888	143	2	2	2563	2847	934	23
16.	2/5/20	1961	14730	1	703	129	1	8	492	320	2271	20
17.	2/1/20	2102	11433	1	440	177	1	0	913	439	358	11
18.	2/5/20	2003	15626	0	1172	167	0	10	470	263	1558	19
19.	2/1/20	2134	12444	1	412	186	1	1	862	551	366	19
20.	2/5/20	1479	12707	0	895	207	1	25	413	136	386	33
21.	2/5/20	1453	11941	0	179	139	1	11	485	174	116	9
22.	2/19/20	2957	12081	1	684	197	2	6	1505	788	688	19
23.	2/17/20	1755	8335	0	785	227	1	4	819	570	1224	29
24.	2/17/20	1215	14889	0	1027	232	1	7	458	335	1506	30
25.	2/17/20	719	14141	0	313	199	1	5	569	284	214	27
26.	2/17/20	5764	22470	0	757	152	1	3	431	534	1511	33
27.	2/17/20	1216	8996	0	179	129	1	5	343	149	78	9

Appendix C - Diel Sampling Results

Table 9 Field measured data and major anions for diel sampling at Mulberry Creek. Units are mg/L for all parameters except T (C), EC (mS), pH and alkalinity (meq/L).

Hour	DO	Temp	EC	pH	F	Cl	Br	NO ₃	SO ₄	Alk
0	6.1	25.0	1.1	8.1	0.3	57.2	0.2	1.8	241.0	5.0
1.5	6.0	25.0	1.1	8.1	0.4	57.4	0.2	1.9	240.3	5.0
3	6.9	25.3	1.1	8.1	0.4	57.5	0.2	1.9	274.1	5.0
4.5	7.7	26.0	1.1	8.1	0.4	58.1	0.2	1.9	249.2	4.9
6	8.4	26.6	1.1	8.2	0.4	60.0	0.2	1.8	348.1	5.0
7.5	8.7	27.0	1.1	8.2	0.4	59.2	0.2	1.9	240.7	5.7
9	8.4	27.0	1.1	8.2	0.4	59.6	0.2	1.8	246.1	5.0
10.5	8.2	27.0	1.1	8.2	0.4	60.4	0.2	1.9	234.4	4.9
12	7.7	28.8	1.1	8.2	0.4	59.7	0.2	1.8	290.2	4.6
13.5	7.3	26.5	1.1	8.2	0.4	60.9	0.2	1.8	237.7	5.0
15	6.9	26.3	1.1	8.2	0.4	60.2	0.2	1.8	237.4	5.1
16.5	6.6	26.1	1.1	8.2	0.4	60.3	0.2	1.8	229.6	5.0
18	6.5	25.8	1.1	8.1	0.4	60.2	0.2	1.7	273.8	4.8
19.5	6.4	25.6	1.1	8.1	0.4	60.9	0.2	1.8	252.9	5.0
21	6.3	25.5	1.1	8.1	0.4	60.5	0.2	1.8	238.3	4.6
22.5	6.2	25.3	1.1	8.1	0.4	60.3	0.2	1.9	244.0	5.0
24	6.3	25.2	1.1	8.1	0.4	61.6	0.2	2.0	234.8	5.1

Table 10 Major cations, nutrients and isotope data for diel sampling at Mulberry Creek. Units are mg/L for all parameters except isotopes, which are permille.

Hour	Na	K	Mg	Ca	Sr	NPOC	TN	Iron	dH ₂	dO ₁₈
0	75.4	5.4	29.9	113.1	3.8	6.4	1.3	1.0	-35.0	-5.2
1.5	77.8	5.1	30.4	110.2	3.8	6.0	1.0	1.4	-35.0	-5.2
3	75.1	5.1	30.4	110.9	3.8	5.7	0.9	2.6	-35.0	-5.3
4.5	75.1	5.3	30.5	111.1	3.7	6.6	1.0	1.9	-35.0	-5.2
6	72.0	5.1	30.5	112.4	3.7	6.5	1.0	1.6	-35.0	-5.2
7.5	100.3	5.0	30.5	110.6	3.8	6.1	0.9	1.2	-35.0	-5.2
9	75.6	5.0	30.5	111.4	4.0	5.5	0.9	1.7	-35.0	-5.2
10.5	73.7	4.9	30.3	106.2	3.9	6.0	1.1	1.6	-35.0	-5.3
12	73.2	5.1	30.1	111.1	3.6	6.6	0.9	2.0	-35.0	-5.3
13.5	73.7	5.1	30.1	110.4	3.6	6.6	1.1	1.8	-35.0	-5.3
15	72.9	5.0	30.3	110.8	3.6	5.6	0.8	0.8	-35.0	-5.3
16.5	74.9	5.0	30.2	113.9	3.6	6.1	1.0	1.4	-35.0	-5.3
18	75.0	5.0	30.2	112.8	3.6	5.4	0.9	1.1	-35.0	-5.3
19.5	76.7	5.2	30.1	109.8	3.5	5.6	0.9	1.5	-35.0	-5.3
21	74.9	5.1	30.2	115.8	3.6	5.6	0.9	1.9	-35.0	-5.3
22.5	80.5	4.9	30.5	107.1	3.7	5.4	0.9	1.5	-36.0	-5.3
24	76.4	5.1	30.4	110.8	3.7	5.2	0.8	1.7	-35.0	-5.3

Table 11 Field measured data and major anions for diel sampling at Chapman Creek. Units are mg/L for all parameters except T (C), EC (mS), pH and alkalinity (meq/L).

Hour	DO	Temp	EC	pH	F	Cl	Br	NO ₃	SO ₄	Alk
0	7.1	20.0	0.7	7.9	0.3	15.6	0.1	5.6	130.6	3.9
1.5	7.4	20.2	0.7	7.9	0.3	15.9	0.1	5.5	128.8	3.9
3	7.3	20.5	0.7	7.9	0.3	15.9	0.1	5.6	120.7	3.9
4.5	7.3	21.2	0.7	8.0	0.4	16.6	0.1	5.5	128.6	4.0
6	7.3	21.8	0.7	8.0	0.3	17.1	0.1	5.8	137.4	4.0
7.5	7.2	22.1	0.7	7.9	0.3	16.5	0.1	5.6	131.8	4.4
9	7.0	22.1	0.7	8.0	0.3	16.7	0.1	5.8	125.9	4.7
10.5	7.0	22.1	0.7	8.0	0.3	16.9	0.1	5.8	140.8	3.6
12	-	-	-	-	-	-	-	-	-	-
13.5	6.8	21.9	0.7	8.0	0.3	18.1	0.1	6.2	146.5	4.2
15	-	-	-	8.0	0.3	17.2	0.1	6.1	151.8	4.2
16.5	6.8	21.6	0.8	8.0	0.3	17.9	0.1	6.2	152.0	3.7
18	6.8	21.3	0.8	8.0	0.3	18.3	0.1	6.5	168.7	3.8
19.5	6.9	21.1	0.8	8.0	0.3	18.3	0.1	6.4	160.7	4.4
21	7.0	20.9	0.8	8.0	0.3	18.6	0.1	6.5	168.1	4.0
22.5	7.0	20.8	0.8	8.0	0.3	19.1	0.1	6.4	173.7	4.5
24	7.1	20.8	0.8	8.0	0.3	19.3	0.1	6.5	169.1	4.4

Table 12 Major cations, nutrients and isotope data for diel sampling at Chapman Creek. Units are mg/L for all parameters except isotopes, which are permille.

Hour	Na	K	Mg	Ca	Sr	NPOC	TN	Iron	dH ₂	dO ₁₈
0	25.9	6.2	44.7	83.7	3.3	3.7	7.7	2.1	-30.0	-5.0
1.5	26.3	6.2	40.6	79.7	3.3	2.7	7.3	2.0	-30.0	-5.0
3	26.3	6.1	39.2	79.4	3.5	3.3	8.4	2.1	-30.0	-5.0
4.5	26.8	6.2	38.5	80.0	3.2	2.7	7.7	2.5	-30.0	-5.0
6	26.9	6.2	40.0	79.4	3.6	3.0	7.5	2.1	-30.0	-5.0
7.5	26.7	6.0	40.1	79.8	3.4	3.0	9.0	2.3	-30.0	-5.0
9	27.4	6.1	42.8	82.6	3.4	3.3	8.9	2.2	-30.0	-5.0
10.5	27.5	6.1	38.3	78.3	3.8	3.0	7.5	2.0	-30.0	-5.0
12	27.3	-	43.4	81.6	3.5	2.8	8.0	2.6	-	-
13.5	27.8	6.0	43.8	83.9	3.5	3.0	8.4	2.2	-30.0	-4.9
15	27.8	6.0	47.0	87.0	3.5	3.0	7.2	2.6	-30.0	-4.9
16.5	28.5	5.9	47.5	87.6	3.8	2.5	7.1	2.6	-30.0	-4.8
18	28.0	6.2	51.2	90.9	4.2	3.2	7.1	2.1	-	-
19.5	28.5	7.8	39.5	80.4	2.3	4.0	8.0	2.2	-	-
21	29.0	5.8	47.0	87.8	3.8	2.2	7.0	2.1	-29.0	-4.7
22.5	28.7	5.9	53.0	93.2	3.3	2.6	7.7	2.3	-	-
24	29.3	5.7	27.0	99.9	4.2	2.5	7.8	2.2	-	-

Table 13 Field measured data and major anions for diel sampling at Vermillion Creek. Units are mg/L for all parameters except T (C), EC (mS), pH and alkalinity (meq/L).

Hour	DO	Temp	EC	pH	F	Cl	Br	NO ₃	SO ₄	Alk
0	7.0	25.0	0.7	8.2	0.3	14.5	0.1	5.7	57.0	5.1
1.5	8.2	25.4	0.7	8.2	0.3	14.7	0.1	5.5	56.9	5.6
3	9.2	26.1	0.6	8.2	0.3	14.2	0.1	5.4	57.2	5.3
4.5	10.8	27.4	0.7	8.3	0.3	15.3	0.1	5.2	56.8	5.4
6	11.8	28.8	0.6	8.4	0.3	14.6	0.1	4.8	56.7	5.2
7.5	11.8	29.3	0.6	8.3	0.3	14.5	0.1	4.9	56.2	5.0
9	10.8	29.0	0.6	8.3	0.3	14.1	0.1	4.6	57.0	5.1
10.5	9.6	28.6	0.6	8.3	0.3	14.4	0.1	4.9	56.1	5.2
12	8.7	28.1	0.6	8.3	0.3	14.3	0.1	4.9	55.4	5.2
13.5	7.8	27.4	0.6	8.3	0.3	14.4	0.1	4.9	56.0	5.2
15	7.5	26.6	0.6	8.3	0.3	14.2	0.1	5.0	55.3	5.2
16.5	7.1	26.0	0.6	8.3	0.3	14.2	0.1	5.0	56.7	5.2
18	6.8	25.6	0.6	8.3	0.3	14.3	0.1	5.1	56.5	5.3
19.5	6.6	25.1	0.7	8.2	0.3	14.3	0.1	5.1	56.7	5.3
21	6.8	24.6	0.7	8.2	0.3	14.0	0.1	5.0	56.0	5.2
22.5	6.7	24.2	0.7	8.2	0.3	13.9	0.1	5.0	58.1	5.3
24	7.2	24.1	0.7	8.2	0.3	14.0	0.1	5.0	56.9	5.4

Table 14 Major cations, nutrients and isotope data for diel sampling at Vermillion Creek. Units are mg/L for all parameters except isotopes, which are permille.

Hour	Na	K	Mg	Ca	Sr	NPOC	TN	Iron	dH ₂	dO ₁₈
0	25.9	6.2	44.7	83.7	3.3	3.7	7.7	2.1	-30.0	-5.0
1.5	26.3	6.2	40.6	79.7	3.3	2.7	7.3	2.0	-30.0	-5.0
3	26.3	6.1	39.2	79.4	3.5	3.3	8.4	2.1	-30.0	-5.0
4.5	26.8	6.2	38.5	80.0	3.2	2.7	7.7	2.5	-30.0	-5.0
6	26.9	6.2	40.0	79.4	3.6	3.0	7.5	2.1	-30.0	-5.0
7.5	26.7	6.0	40.1	79.8	3.4	3.0	9.0	2.3	-30.0	-5.0
9	27.4	6.1	42.8	82.6	3.4	3.3	8.9	2.2	-30.0	-5.0
10.5	27.5	6.1	38.3	78.3	3.8	3.0	7.5	2.0	-30.0	-5.0
12	27.3	-	43.4	81.6	3.5	2.8	8.0	2.6	-	-
13.5	27.8	6.0	43.8	83.9	3.5	3.0	8.4	2.2	-30.0	-4.9
15	27.8	6.0	47.0	87.0	3.5	3.0	7.2	2.6	-30.0	-4.9
16.5	28.5	5.9	47.5	87.6	3.8	2.5	7.1	2.6	-30.0	-4.8
18	28.0	6.2	51.2	90.9	4.2	3.2	7.1	2.1	-	-
19.5	28.5	7.8	39.5	80.4	2.3	4.0	8.0	2.2	-	-
21	29.0	5.8	47.0	87.8	3.8	2.2	7.0	2.1	-29.0	-4.7
22.5	28.7	5.9	53.0	93.2	3.3	2.6	7.7	2.3	-	-
24	29.3	5.7	27.0	99.9	4.2	2.5	7.8	2.2	-	-

Table 15 Field measured data and major anions for diel sampling at Mill Creek. Units are mg/L for all parameters except T (C), EC (mS), pH and alkalinity (meq/L).

Hour	F	Cl	Br	NO ₃	SO ₄	DO	Temp	EC	pH	Alk
0	0.3	8.0	0.0	5.2	38.2	7.4	24.5	0.6	8.2	5.2
1.5	0.2	8.2	0.0	5.1	37.0	7.3	24.5	0.6	8.1	5.3
3	0.2	8.1	0.1	5.5	40.5	7.4	24.7	0.6	8.1	5.3
4.5	0.2	7.9	0.0	5.5	40.3	7.6	24.9	0.6	8.1	5.4
6	0.2	7.9	0.0	5.4	39.3	7.6	25.2	0.6	8.1	5.4
7.5	0.2	8.0	0.0	5.5	40.3	7.8	25.4	0.6	8.1	5.3
9	0.2	9.3	0.0	5.5	39.7	7.9	25.4	0.6	8.1	5.4
10.5	0.2	8.9	0.0	5.5	39.6	7.7	25.3	0.6	8.2	5.0
12	0.2	8.3	0.0	5.6	41.1	7.6	25.2	0.6	8.2	5.4
13.5	0.3	10.6	0.0	5.7	41.4	7.5	25.0	0.6	8.2	5.3
15	0.2	8.1	0.0	5.5	40.4	7.6	24.8	0.6	8.2	5.4
16.5	0.2	8.2	0.0	5.7	42.1	7.3	24.6	0.6	8.2	5.5
18	0.2	8.0	0.0	5.8	41.7	7.2	24.4	0.6	8.2	5.5
19.5	0.2	8.3	0.1	5.8	43.4	7.2	24.3	0.6	8.2	4.7
21	0.2	8.8	0.0	5.8	43.5	7.2	24.2	0.6	8.2	5.5
22.5	0.2	8.4	0.1	5.8	43.8	7.2	24.1	0.6	8.2	5.4
24	0.2	8.4	0.1	5.8	44.1	7.2	24.0	0.6	8.2	5.6

Table 16 Major cations, nutrients and isotope data for diel sampling at Mill Creek. Units are mg/L for all parameters except isotopes, which are permille.

Hour	Na	K	Mg	Ca	Sr	NPOC	TN	Iron	dH ₂	dO ₁₈
0	8.3	3.1	16.7	89.2	3.4	2.8	1.5	1.6	-30.0	-5.0
1.5	8.2	3.0	16.8	86.1	3.4	2.4	1.5	1.4	-31.0	-5.0
3	8.3	3.0	17.0	88.1	3.5	2.3	1.5	2.1	-31.0	-5.0
4.5	8.2	3.0	17.0	87.4	3.5	2.2	1.6	1.9	-31.0	-5.0
6	8.4	3.1	17.1	90.1	3.5	2.3	1.5	1.6	-31.0	-5.1
7.5	8.6	3.3	16.9	84.3	3.5	2.6	1.5	1.8	-31.0	-5.0
9	9.0	3.4	17.2	89.5	3.6	2.5	1.5	1.6	-31.0	-5.0
10.5	8.5	3.1	17.0	89.8	3.6	3.3	1.5	2.1	-31.0	-5.1
12	8.6	3.1	17.3	89.0	3.7	3.0	1.5	1.6	-31.0	-5.1
13.5	8.4	3.0	17.1	90.6	3.6	2.8	1.6	1.6	-31.0	-5.0
15	8.7	3.1	17.3	91.7	3.7	2.6	1.5	1.6	-31.0	-5.0
16.5	9.2	3.4	17.4	86.0	3.8	2.1	1.5	1.6	-31.0	-5.1
18	8.8	3.1	17.5	92.2	3.8	2.4	1.5	1.2	-30.0	-4.9
19.5	9.0	3.4	17.5	90.4	3.8	2.2	1.5	2.2	-28.0	-3.9
21	8.7	3.1	17.5	91.6	3.7	2.3	1.6	2.3	-31.0	-5.1
22.5	8.9	3.0	17.6	91.4	3.8	2.8	1.6	1.2	-28.0	-4.0
24	9.2	3.4	17.7	92.0	3.7	2.5	1.5	1.7	-29.0	-4.6

Appendix D - Groundwater Data

Table 17 Information and field data from groundwater sampling. Measurements were taken approximately 10 minutes apart. Samples were taken after the last measurement was recorded.

Site	Mulberry	Chapman	Vermillion	Mill
Sample Date	2/3/2020	11/01/2019	7/11/2019	11/08/2019
Time 1				
DO (mg/L)	0.3	0.2	7.2	0.3
pH	6.63	7.13	7.04	7.01
EC (mS)	0.7065	1.418	0.986	1.179
Temp (C)	14.4	14	19.4	14.75
Time 2				
DO (mg/L)	0.2	0.1	6.5	0.1
pH	6.43	7.14	7.04	7.01
EC (mS)	0.703	1.4185	0.9845	1.1755
Temp (C)	14.5	14.6	18.5	14.85
Time 3				
DO (mg/L)	0.1		6.3	0.5
pH	6.5	7.14	7.04	6.99
EC (mS)	0.704	1.4165	0.982	1.194
Temp (C)	14.5	15.1	18	14.8
Time 4				
DO (mg/L)	0.1	0.2	6.3	-
pH	6.6	7.14	7.04	-
EC (mS)	0.693	1.4165	0.988	-
Temp (C)	14.5	15.1	17.9	-

Table 18 Average groundwater geochemical results. Units are mg/L for all parameters except T (C), EC (mS), pH, alkalinity (meq/L) and isotopes (permille).

	Vermillion	Chapman	Mill	Mulberry
DO	6.3	0.3	0.5	0.1
Temp	17.9	14.5	14.8	14.5
EC	1	1.4	1.2	0.7
pH	7	7.1	7	6.6
F	0.3	0.2	0.2	0.4
Cl	18.2	78.8	73.4	23.8
Br	0.1	0.3	0.4	0.2
NO₃	79.7	0.1	27.6	4.5
SO₄	85.1	326.1	88.2	-
Alk	6.7	6.6	7.3	5.1
Na	77.3	60.3	104.7	25
K	2	3.3	1.7	2
Mg	18	58	20.5	-
Ca	103.8	155	117.2	49.5
Sr	3.6	8.7	3.4	
OP	0	0	0	1.2
Iron	1.2	6.2	1	0
NPOC	1.5	1.8	2.5	0.8
TN	22.3	1.2	7.6	1
d₂H	-31	-40	-36	-41
d₁₈O	-5	-6.1	-5.9	-6.3

Appendix E - WS Characteristics (Prism and GAGES II Data)

Table 19 The following tables provide data gathered from online databases and used in our statistical analyses. Annual precipitation and temperature were from Prism, all other information was gathered from USGS GAGES II. Continued onto following pages.

Site	DA	Annual PPT	Annual Temp	Agriculture	Grassland	Urban	Forest	Total flow (km)
1	341.00	607.74	11.60	67.64	31.38	0.00	0.94	1266.01
2	227.00	692.33	13.10	48.82	47.73	0.12	3.19	976.18
3	406.00	748.91	11.20	43.45	53.90	0.07	1.75	1975.35
4	261.00	780.10	13.20	20.50	77.61	0.19	1.55	1220.27
5	86.00	852.27	13.80	79.59	10.08	7.84	1.82	385.13
6	300.00	822.19	12.90	39.01	57.72	0.26	2.80	1443.58
7	344.00	821.08	11.90	48.06	46.36	0.64	4.71	1666.50
8	426.00	922.76	13.80	55.07	38.93	0.43	4.70	1957.70
9	110.00	873.33	13.10	9.04	87.97	0.16	2.40	590.51
10	410.00	849.62	11.90	64.54	28.81	0.72	5.23	1922.07
11	445.00	1029.67	14.60	0.00	0.00	0.00	0.00	0.00
12	243.00	876.28	12.60	23.02	64.65	0.42	11.47	1067.61
13	220.00	1059.66	13.90	6.72	85.17	0.56	6.05	989.04
14	318.00	907.85	12.70	6.58	86.28	0.28	6.48	1373.00
15	276.00	840.59	11.50	38.52	49.79	0.04	11.27	1164.83
16	177.00	961.79	12.80	14.43	79.81	0.00	5.34	503.49
17	149.00	922.88	12.70	22.00	65.80	0.00	11.78	656.77
18	114.00	986.09	12.80	19.81	71.13	0.70	8.05	533.39
19	290.00	939.90	12.90	22.86	64.83	0.77	10.99	1271.68
20	97.80	977.31	12.70	28.98	61.80	1.39	7.21	441.95
21	164.00	957.06	12.60	16.51	66.39	1.31	14.55	748.12
22	431.00	926.58	12.50	48.30	44.01	0.99	6.06	1523.92
23	406.00	1007.97	12.60	35.50	46.97	0.79	16.09	1598.10
24	28.70	1033.55	12.80	34.47	50.17	5.37	8.69	118.13
25	53.40	1017.12	12.70	17.55	47.41	16.44	17.34	151.61
26	58.10	1027.41	13.00	1.95	19.27	67.27	10.26	213.84
27	65.80	1041.02	13.00	13.35	49.94	20.99	14.51	306.79

Site	Basin Comp	PET	Clay	Silt	Sand	Elev.	Slope	Pop Den
1	0.37	766.88	21.33	69.06	9.61	745.87	1.70	0.16
2	1.38	746.89	25.65	64.42	9.93	564.30	2.46	0.78
3	1.73	816.86	29.65	56.97	13.38	447.26	2.72	0.44
4	1.87	821.86	27.26	50.06	22.68	437.96	3.37	1.86
5	2.28	848.50	28.98	43.29	27.73	434.10	0.94	35.33
6	1.50	820.44	30.05	54.77	15.19	401.12	2.20	1.89
7	1.68	779.08	31.20	56.49	12.32	451.51	2.34	3.06
8	2.24	824.32	39.36	51.11	9.53	435.28	1.73	0.41
9	1.70	785.88	38.11	47.24	14.65	398.91	2.52	3.65
10	1.59	861.76	37.03	53.24	9.73	343.27	3.75	1.12
11	1.86	792.97	36.77	49.33	13.90	379.19	3.74	2.97
12	2.04	847.56	37.95	52.77	9.28	355.87	2.82	1.82
13	2.08	785.13	40.40	49.80	9.80	397.55	4.61	2.84
14	1.51	794.25	35.61	48.60	15.79	396.36	3.30	2.36
15	2.17	785.36	39.92	51.13	8.94	386.45	2.32	1.50
16	1.32	796.11	37.83	47.94	14.24	360.83	3.23	2.14
17	2.10	787.98	39.25	51.52	9.22	367.50	2.73	4.94
18	1.20	798.81	37.38	48.36	14.26	340.86	3.23	7.07
19	1.35	813.52	38.90	53.09	8.02	341.44	2.06	8.42
20	1.24	812.64	38.82	52.99	8.18	339.19	2.14	9.92
21	1.47	796.14	38.92	50.87	10.20	336.80	2.81	20.55
22	1.58	796.53	36.71	49.29	14.00	349.09	2.65	6.17
23	1.42	801.72	35.32	51.27	13.41	314.57	3.32	11.94
24	2.04	815.37	36.31	53.49	10.20	312.14	1.52	43.28
25	1.97	814.30	36.69	54.41	8.90	295.22	2.28	54.69
26	1.89	809.34	36.28	58.83	4.89	294.28	3.64	464.57
27	2.40	802.37	37.49	57.17	5.35	313.73	2.55	66.95

Site	Developed	Forest NLCD06	Plant NLCD06	Grass NLCD06	Pasture NLCD06	Crop NLCD06
1	3.28	0.28	61.96	32.84	0.00	61.96
2	4.12	3.83	45.83	45.01	0.05	45.78
3	3.24	1.91	41.35	52.49	0.55	40.80
4	4.26	3.35	19.67	71.35	1.18	18.48
5	7.85	1.64	74.00	15.00	1.20	72.79
6	3.96	4.80	33.50	56.77	0.90	32.60
7	4.69	5.59	46.94	42.26	1.98	44.95
8	2.64	2.76	10.47	82.14	3.05	7.42
9	4.63	6.55	60.20	27.28	2.61	57.59
10	3.16	5.25	18.32	72.41	14.35	3.96
11	4.14	12.08	27.61	55.22	9.38	18.22
12	2.97	5.33	26.94	63.05	22.63	4.31
13	3.23	4.11	13.34	78.51	8.75	4.59
14	3.72	14.48	36.04	44.54	9.97	26.06
15	3.67	3.43	21.69	69.90	12.90	8.78
16	3.55	8.46	60.29	26.21	44.43	15.86
17	5.19	5.87	34.24	53.72	20.76	13.49
18	4.64	9.12	61.87	22.84	43.95	17.91
19	5.10	5.76	40.13	48.17	20.54	19.59
20	5.51	5.88	38.91	48.75	20.17	18.74
21	6.70	11.87	47.67	31.42	36.42	11.25
22	4.94	8.42	74.92	10.07	36.62	38.30
23	5.51	16.70	72.72	3.35	47.11	25.61
24	13.85	5.54	78.49	0.79	42.98	35.51
25	30.88	12.28	53.40	1.68	30.75	22.65
26	62.77	11.75	22.11	2.16	15.94	6.16
27	23.40	10.48	62.75	1.42	42.63	20.12

Site	NAppKG sqKM	PhosAppKG sqKM	PestAppKG sqKM	Screening Comments
1	3832.49	648.32	66.40	hvy irrigated ag, small towns
2	3524.62	591.41	47.33	hvy ag, NEoA
3	4269.83	707.87	38.19	hvy ag, NEoA
4	2629.69	495.21	15.08	hvy ag, forest rip, lt develop, NEoA
5	7043.21	973.54	64.46	urban
6	4797.07	805.07	41.36	hvy ag, small towns, NEoA
7	6104.13	1051.23	72.15	hvy ag, NEoA
8	2422.31	522.34	13.80	hvy ag, NEoA
9	5823.46	932.19	83.48	hvy ag, much riparian, NEoA
10	2061.03	503.09	6.75	small dams on most tribs
11	4521.84	864.28	47.39	hvy ag in valleys, no ag in uplands, NEoA
12	2154.90	478.48	10.13	small dams on most tribs
13	2241.11	483.55	13.24	hvy ag, small reservoirs on some tribs, NEoA
14	4534.49	786.57	69.54	hvy ag, some riparian, NEoA
15	2921.79	580.86	26.13	hvy ag, some riparian, NEoA
16	3988.58	737.16	37.69	hvy ag, some riparian, NEoA
17	3393.59	622.05	41.46	hvy ag, NEoA
18	3844.81	690.89	42.16	hvy ag, much riparian, NEoA
19	3506.59	585.71	56.61	hvy ag, some riparian, upstrm city, NEoA
20	3395.91	569.77	54.23	hvy ag, some riparian, upstrm city, NEoA
21	3254.95	544.53	39.81	hvy ag, forest rip, lt develop, NEoA
22	6336.18	1026.44	84.63	upstrm towns & small reservoirs
23	5420.31	904.62	66.61	hvy ag, much riparian, NEoA
24	4740.01	766.36	48.37	hvy ag, forest rip, channeled hw, upstrm towns, imoundment on prox trib
25	4120.74	662.96	30.82	ag, forested rip, suburban, small impoundments
26	3293.11	528.08	15.02	ag, forested rip, suburban, small impoundments
27	4251.65	689.49	30.38	ag, forested rip, suburban, small impoundments

Site	Corn	Sorghum	Soybeans	Pasture	WinterWheat	Wwht_Soy	AvgCrops
1	19.73	7.66	3.46	32.93	17.70	0.05	81.53
2	4.65	9.43	12.25	42.06	17.79	0.23	86.42
3	1.18	7.34	4.64	51.73	24.18	0.37	89.44
4	0.28	2.36	2.28	68.58	11.76	0.73	85.98
5	5.65	8.89	11.65	11.77	37.68	5.38	81.02
6	1.23	7.87	9.16	50.75	14.34	2.58	85.94
7	8.61	6.36	15.66	38.63	12.64	0.68	82.57
8	1.73	0.53	2.05	64.53	1.36	0.20	70.39
9	21.19	0.97	26.36	14.11	7.22	0.29	70.14
10	0.25	0.03	0.61	28.09	0.49	0.11	29.57
11	8.46	0.25	8.05	21.93	0.67	0.07	39.43
12	1.27	0.20	2.52	22.05	0.40	0.15	26.59
13	1.74	0.12	1.88	20.38	0.33	0.03	24.49
14	10.33	0.28	9.70	5.79	1.91	0.03	28.04
15	4.40	0.13	4.81	32.15	0.13	0.06	41.68
16	7.42	0.28	8.13	11.35	0.39	0.03	27.60
17	4.75	0.25	7.15	16.62	0.65	0.28	29.71
18	7.23	0.41	8.88	8.00	0.62	0.03	25.16
19	6.93	0.41	14.58	22.20	0.59	1.18	45.88
20	6.84	0.37	13.65	21.76	0.55	1.05	44.22
21	5.66	0.18	6.58	9.09	0.32	0.07	21.90
22	20.09	0.14	18.91	7.85	1.37	0.06	48.42
23	13.44	0.03	14.05	0.80	0.28	0.08	28.68
24	9.83	0.22	17.83	0.62	0.52	0.12	29.13
25	3.62	0.01	8.64	0.84	0.45	0.15	13.72
26	0.60	0.01	0.78	0.30	0.02	0.00	1.72
27	1.98	0.02	6.65	0.33	0.38	1.40	10.77

Site	GEOL_Hunt
1	Pliocene-age and older stream deposits on the Great Plains
2	Deeply weathered loess
3	Shaley or sandy ground; on mixed sandstone and shale formations; where shaley, contains considerable swelling clay
4	Sandy or silty residuum; probably includes loess. Depth generally less than 10 feet
5	Sandy or silty residuum; probably includes loess. Depth generally less than 10 feet
6	Deeply weathered loess
7	Deeply weathered loess
8	Sandy or silty residuum; probably includes loess. Depth generally less than 10 feet
9	Pre-Wisconsinan drift
10	Sandy or silty residuum; probably includes loess. Depth generally less than 10 feet
11	Pre-Wisconsinan drift
12	Sandy or silty residuum; probably includes loess. Depth generally less than 10 feet
13	Sandy or silty residuum; probably includes loess. Depth generally less than 10 feet
14	Pre-Wisconsinan drift
15	Sandy or silty residuum; probably includes loess. Depth generally less than 10 feet
16	Wisconsinan loess
17	Sandy or silty residuum; probably includes loess. Depth generally less than 10 feet
18	Wisconsinan loess
19	Sandy or silty residuum; probably includes loess. Depth generally less than 10 feet
20	Sandy or silty residuum; probably includes loess. Depth generally less than 10 feet
21	Sandy or silty residuum; probably includes loess. Depth generally less than 10 feet
22	Wisconsinan loess
23	Wisconsinan loess
24	Wisconsinan loess
25	Wisconsinan loess
26	Pre-Wisconsinan drift
27	Wisconsinan loess

Appendix F - Statistics

Table 20 Results of spearman's rank correlation (rho) listed in table between site characteristics (hydrograph separation, GAGES II and Prism data) and grab sampling data. Italicized numbers represent $P < 0.05$. Bold represents $P < 0.01$. Bold and italicized represents $P < 0.005$. Land use is presented as % Ag (agriculture) and % Dev. (developed).

	Longitude	BFI	BF	RO	% Ag.	% Dev.	PPT	% clay	Temp.
pH	0.19	-0.15	0.26	0.28	-0.12	0.12	0.21	0.49	0.16
DO	0.21	0.01	0.30	0.31	-0.12	<i>0.42</i>	0.17	0.13	<i>0.48</i>
EC	-0.28	0.04	<i>-0.46</i>	-0.27	<i>0.49</i>	0.01	<i>-0.37</i>	-0.56	-0.05
Alk	-0.58	0.53	<i>-0.45</i>	-0.66	<i>0.47</i>	-0.60	-0.63	-0.19	-0.31
F	-0.71	0.52	-0.53	-0.80	<i>0.48</i>	-0.56	-0.84	-0.26	-0.20
Cl	-0.06	-0.12	-0.33	-0.06	<i>0.46</i>	0.31	-0.16	-0.57	-0.03
Br	-0.29	0.06	<i>-0.47</i>	-0.25	0.61	0.09	<i>-0.38</i>	-0.55	-0.03
NO ₃	-0.19	0.16	<i>-0.43</i>	<i>-0.40</i>	0.72	-0.23	-0.23	-0.17	<i>-0.42</i>
SO ₄	-0.52	0.02	-0.76	-0.50	0.56	-0.19	-0.58	<i>-0.44</i>	-0.08
TN	-0.23	-0.09	<i>-0.49</i>	-0.35	0.80	-0.32	-0.39	-0.02	-0.37
NPOC	-0.12	-0.29	<i>-0.44</i>	-0.26	<i>0.57</i>	0.11	-0.20	-0.16	-0.23
Li	-0.78	<i>0.45</i>	-0.69	-0.81	0.59	-0.50	-0.88	<i>-0.48</i>	-0.16
B	-0.64	0.17	-0.70	-0.57	0.57	-0.33	-0.65	<i>-0.49</i>	-0.03
Na	-0.22	-0.10	-0.50	-0.21	0.52	0.18	-0.33	-0.56	-0.03
Mg	-0.65	0.29	-0.53	-0.62	<i>0.44</i>	-0.51	-0.71	-0.28	0.04
P	-0.60	<i>0.48</i>	-0.64	-0.70	0.59	<i>-0.43</i>	-0.72	<i>-0.41</i>	-0.49
S	-0.52	0.02	-0.75	-0.49	0.57	-0.20	-0.57	<i>-0.47</i>	-0.08
K	<i>-0.48</i>	0.12	-0.67	-0.53	0.69	-0.04	-0.59	-0.60	-0.16
Ca	-0.54	0.38	<i>-0.50</i>	<i>-0.49</i>	<i>0.45</i>	-0.33	-0.58	-0.57	-0.08
V	-0.81	<i>0.48</i>	-0.72	-0.86	0.73	-0.55	-0.91	-0.38	-0.25
Mn	-0.26	-0.24	-0.56	-0.33	0.56	0.00	-0.36	-0.45	-0.06
Fe	0.02	<i>-0.47</i>	-0.28	0.03	0.34	-0.03	-0.05	-0.08	-0.06
Ni	<i>-0.41</i>	-0.16	-0.72	<i>-0.45</i>	0.77	-0.19	-0.51	-0.39	-0.23
Co	-0.37	-0.16	-0.68	<i>-0.44</i>	0.76	0.04	-0.50	-0.53	-0.14
Cu	-0.10	0.13	-0.20	-0.35	<i>0.44</i>	-0.31	<i>-0.43</i>	0.06	<i>-0.46</i>
Zn	-0.03	-0.13	-0.18	0.07	0.10	-0.08	0.14	-0.01	-0.03
As	-0.63	<i>0.38</i>	-0.70	-0.83	0.83	<i>-0.45</i>	-0.87	-0.35	<i>-0.49</i>
Se	-0.56	0.39	-0.64	-0.76	0.77	<i>-0.43</i>	-0.78	<i>-0.44</i>	<i>-0.43</i>
Mo	<i>-0.49</i>	0.12	0.58	-0.44	0.61	-0.27	-0.53	<i>-0.49</i>	-0.20
Cd	-0.25	-0.16	-0.51	-0.33	0.51	-0.01	-0.40	-0.51	-0.14
Longitude	-	-0.51	0.68	0.80	<i>-0.48</i>	0.66	0.82	<i>0.42</i>	-0.06
PPT	0.82	<i>-0.44</i>	0.77	0.95	-0.63	0.47	-	<i>0.46</i>	0.34

Appendix G - Detection Limits

Table 21 Detection limits for IC. Units are mg/L.

ICS-1100 Ion Chromatograph (IC)	F	Cl	Br-	NO₃	SO₄2	Na	K	Mg	Ca	Sr
MDL	0.06	1.54	0.08	0.016	0.71	0.22	0.16	0.19	0.50	0.17

Table 22 Detection limit for ICP-MS. Samples were run at 0.9-fold dilution (spiked with 10% v/v of 50 ppb Ga final concentration) as internal standard.

Agilent 7500 ex ICP-MS	Li / 7	B / 11	Na / 23	Mg / 24	P / 31	S / 34	K / 39	Ca / 40	V / 51	Cr / 52
Units	ppt	ppt	ppm	ppb	ppm	ppm	ppm	ppb	ppb	ppb
DL	108	474	0.0064	0.88	0.023	0.21	0.0029	1.28	0.36	0.14
	Mn / 55	Fe / 56	Co / 59	Ni / 60	Cu / 63	Zn / 66	As / 75	Se / 78	Mo / 95	Cd / 111
Units	ppb	ppb	ppt	ppt	ppb	ppb	ppt	ppt	ppt	ppt
DL	0.002 3	0.21	9.18	326	0.052	0.36	33.5	62.7	64.9	18

Appendix H - Ferrozine Protocol

This ferrozine method can only measure the concentration of ferrous iron [Fe(II)]. It is insensitive to ferric iron [Fe(III)]. In order to use the ferrozine method to measure the total concentration of iron in a sample that contains ferric iron, therefore, the ferric iron must first be reduced to ferrous iron.

Reagents:

- 0.5 N HCl.
- 6 M hydroxylamine hydrochloride ($\text{NH}_2\text{OH}\cdot\text{HCl}$; FW = 69.49 g/mol). Do not make a large volume of this reagent. Just make slightly more than you need. It should be used soon after it is made.

Procedure:

1. Add 1 mL of acidified water sample to a 15 mL centrifuge tube. You can use an unacidified sample as well. However, in that case, the ferric iron may not all be dissolved/suspended. Use a sample that was acidified in the field if given the choice and be sure to mix the sample before removing the 1 mL aliquot.
2. Add 0.5 mL of hydroxylamine solution.
3. Add 8.5 mL of 0.5 N HCl. Be careful when pipetting acid. You do not want to draw the solution too rapidly into the pipet. If that happens, acid may splash inside the pipet and damage seals.
4. Cap and vortex the tube and then allow it to incubate overnight.
5. The next day, measure iron concentration in the sample using the ferrozine method (see lab protocol). Note that this digestion dilutes the sample 10-fold. Also note that you will probably want to use a more strongly buffered ferrozine solution. Color development in the assay is pH dependent.

Iron Analysis: Extra-buffering approach

Use this method to analyze the Fe(II) content of samples that have been prepped as outlines above..

Reagents:

- Ferrozine solution –Because the formation of the ferrous-ferrozine complex is pH dependent, some buffering needs to be present to ensure consistency between samples and standards. For this purpose, the standard ferrozine solution contains 46 mM HEPES. For samples from 0.5 N HCl extractions, however, more buffering is needed. Make the ferrozine solution as described above but with 1 M HEPES. Per L of solution: 238.3 g of HEPES, 1 g of ferrozine. Adjust the pH to 7.0 and store at 4°C.
- Ferrous iron standards – Make the standards as described above, except make the dilutions with 0.5 N HCl.
- 0.5 N HCl – Partially fill a 1 L volumetric flask with DI water. Inside a fume hood, slowly add 41.7 mL of concentrated HCl (12 N) to the flask, and then fill the flask to the mark with DI.

Procedure:

1. Add 2.5 mL of ferrozine reagent to a test tube.
2. Add 1 mL of sample/standard and wait for color development. Wait 1 hour and start analyzing samples. You need to be consistent between samples and standards because absorbance changes over time. Therefore, I suggest you work only with small batches of samples (e.g., <20). It may be necessary to dilute the sample (e.g., add 0.1 mL of sample + 0.9 mL of 0.5 N HCl for 1:10 dilution).
3. Set wavelength on spectrophotometer to 562 nm.
4. Normalize absorbance on the spectrophotometer to absorbance of a blank sample consisting of 2.5 mL of ferrozine solution + 1 mL of 0.5 N HCl. Pour the blank sample into a cuvette, place the cuvette in the spectrophotometer, close the lid, and press "Measure Blank".
5. Measure and record the absorbance for each sample/standard. To accomplish this task, you simply add the sample/standard to a cuvette, place it in the spectrophotometer, close the lid, and read the absorbance value on the display.
6. Perform a linear regression on the absorbance and concentration data from the standards. Use this regression line and the absorbance of the samples to calculate sample concentrations.

Appendix I - Extra Figures

Diel Graphs

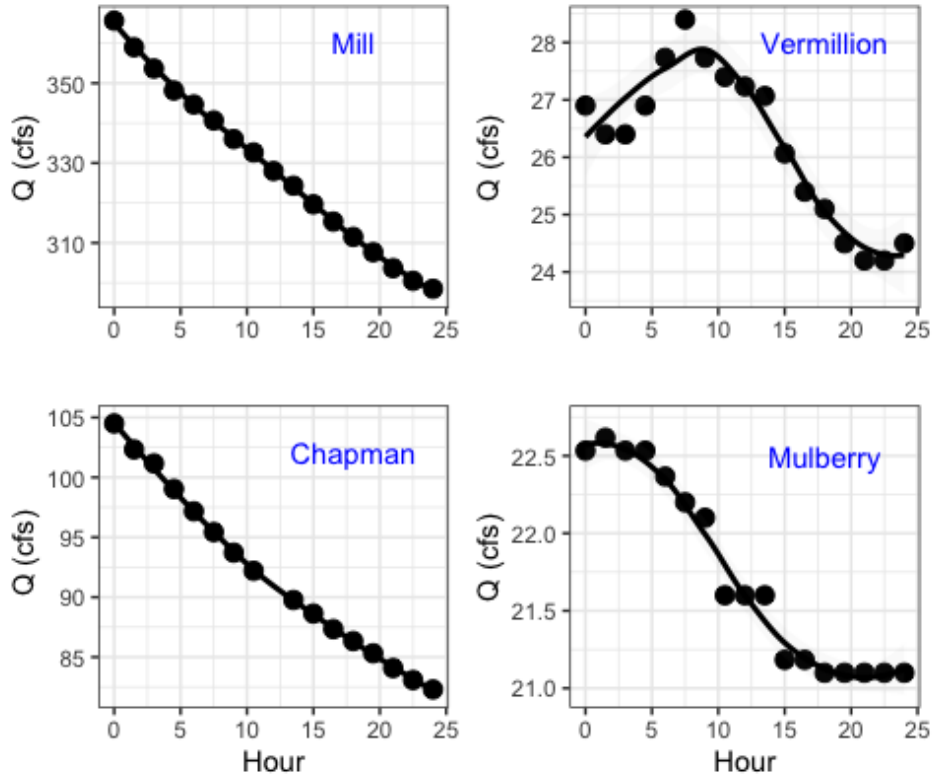
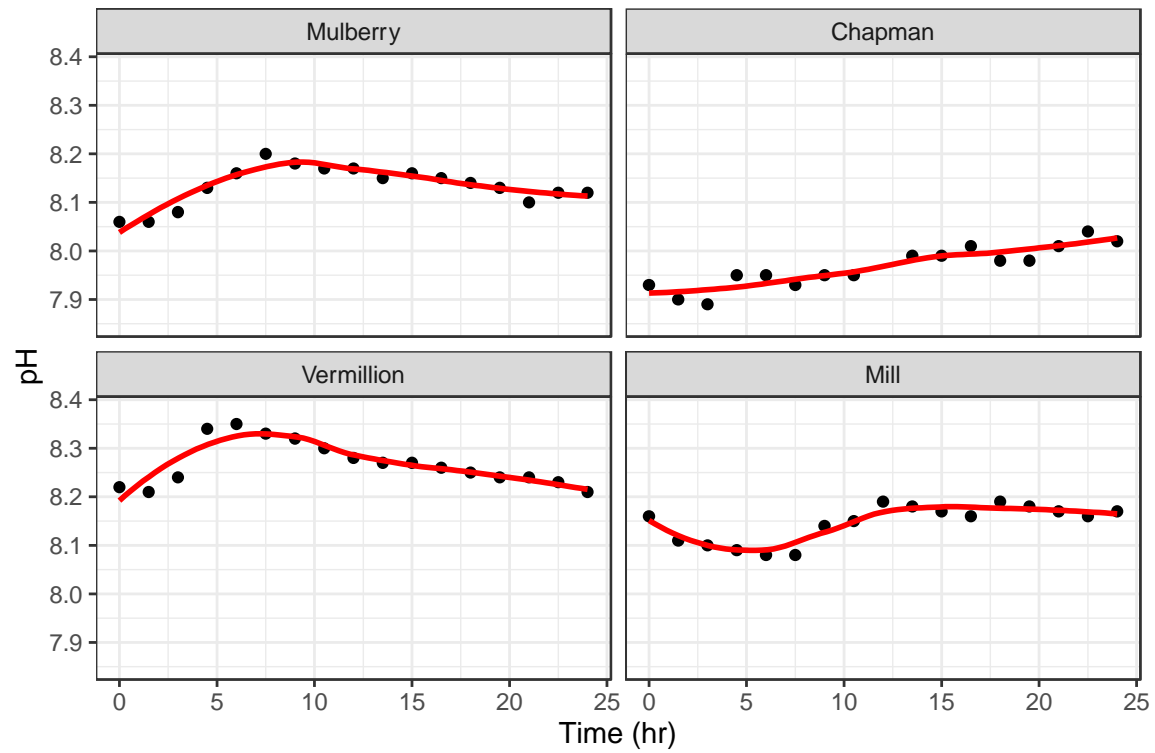
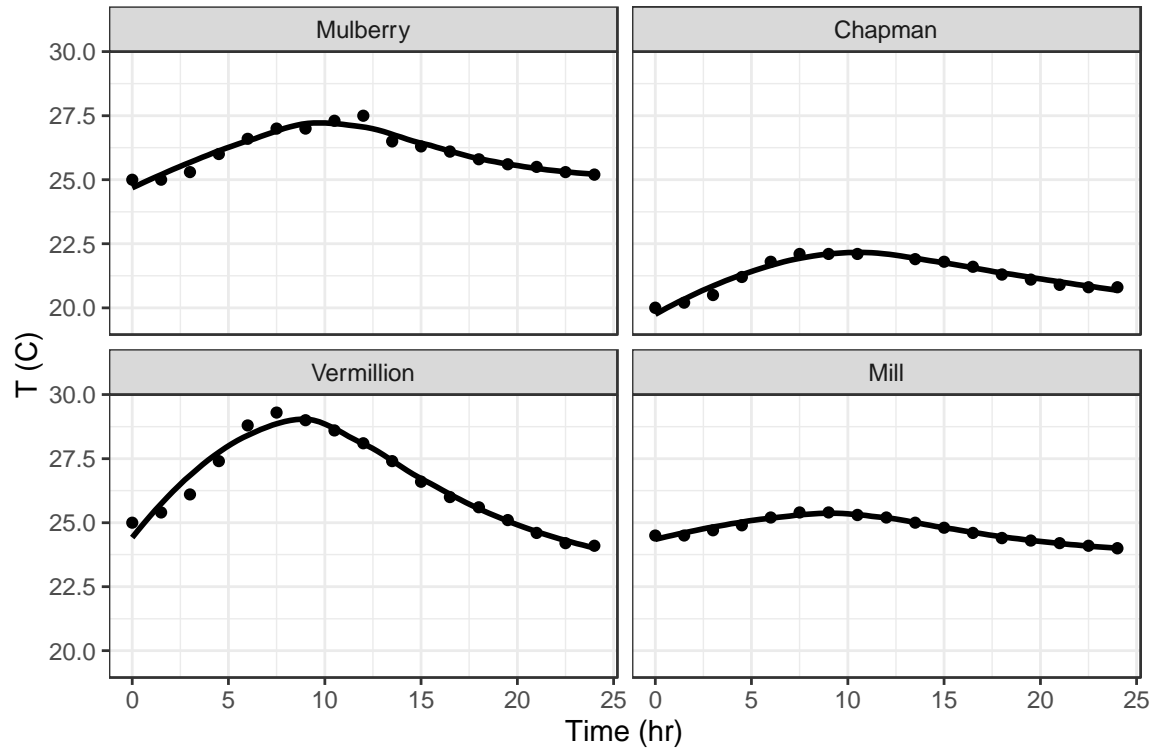
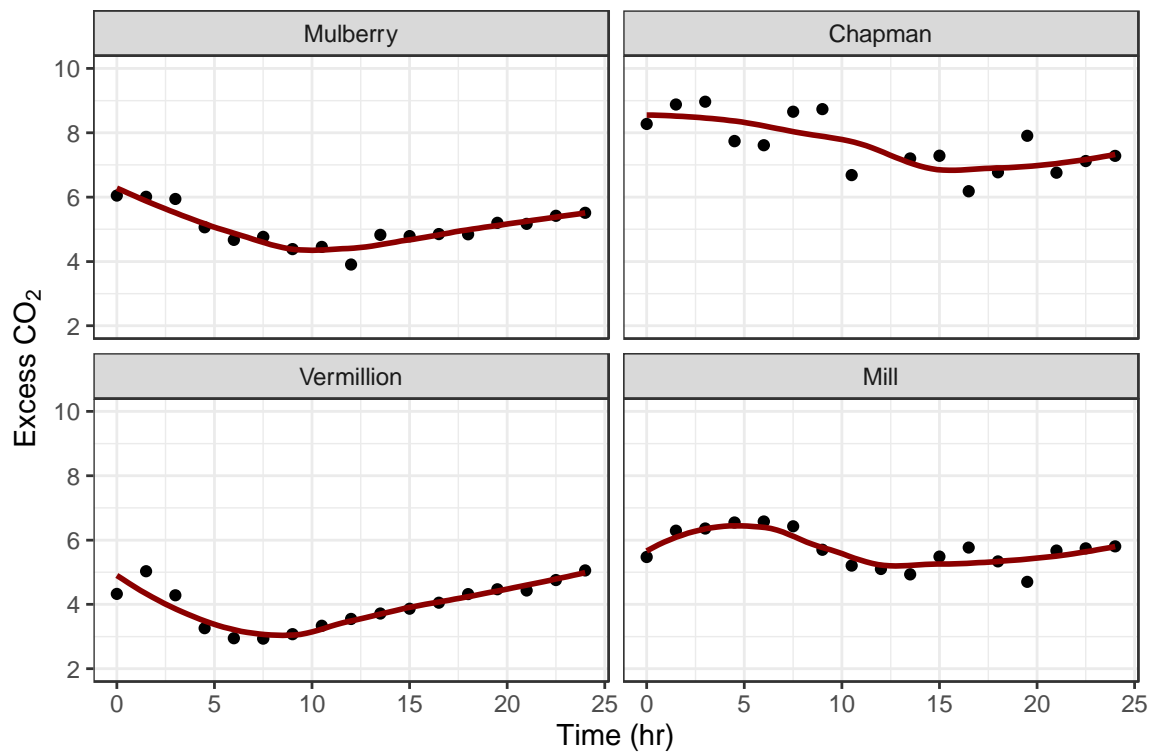
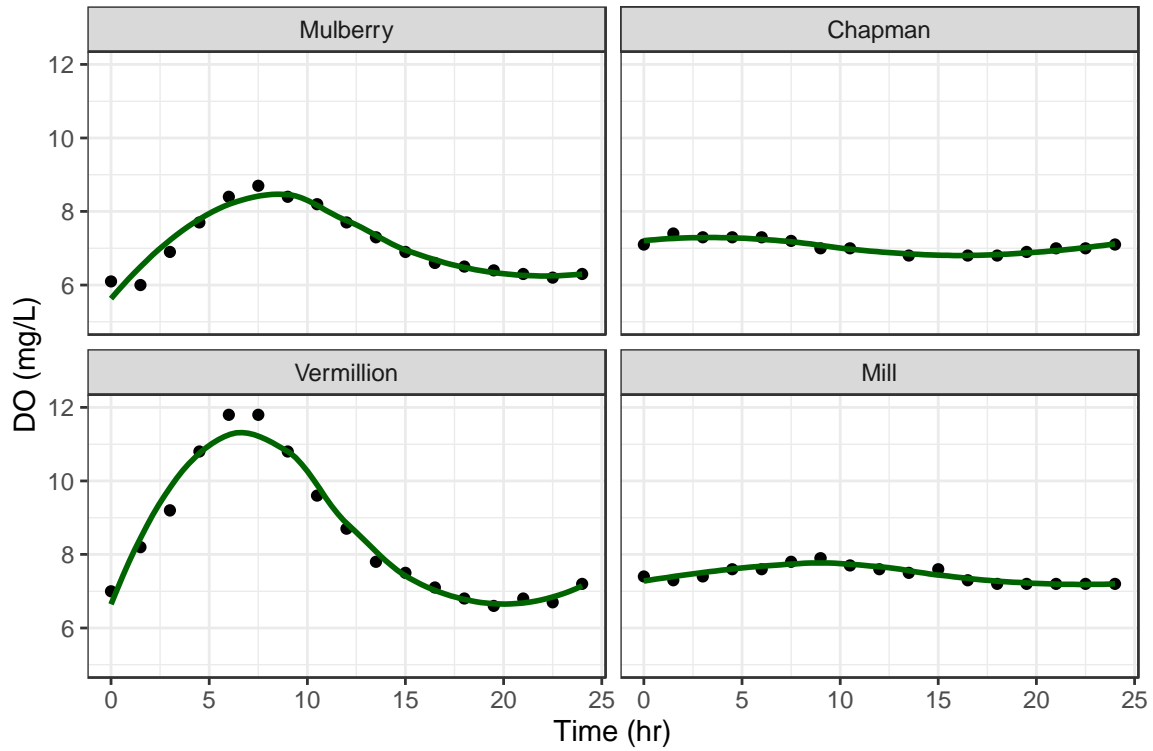
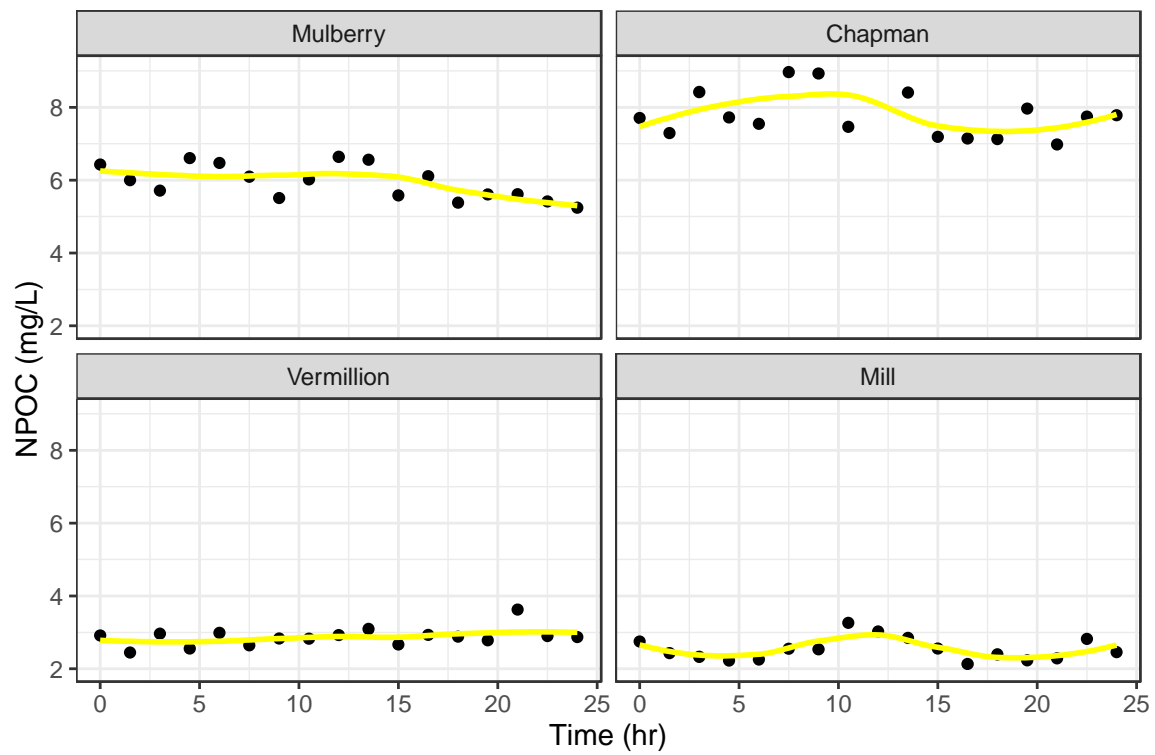
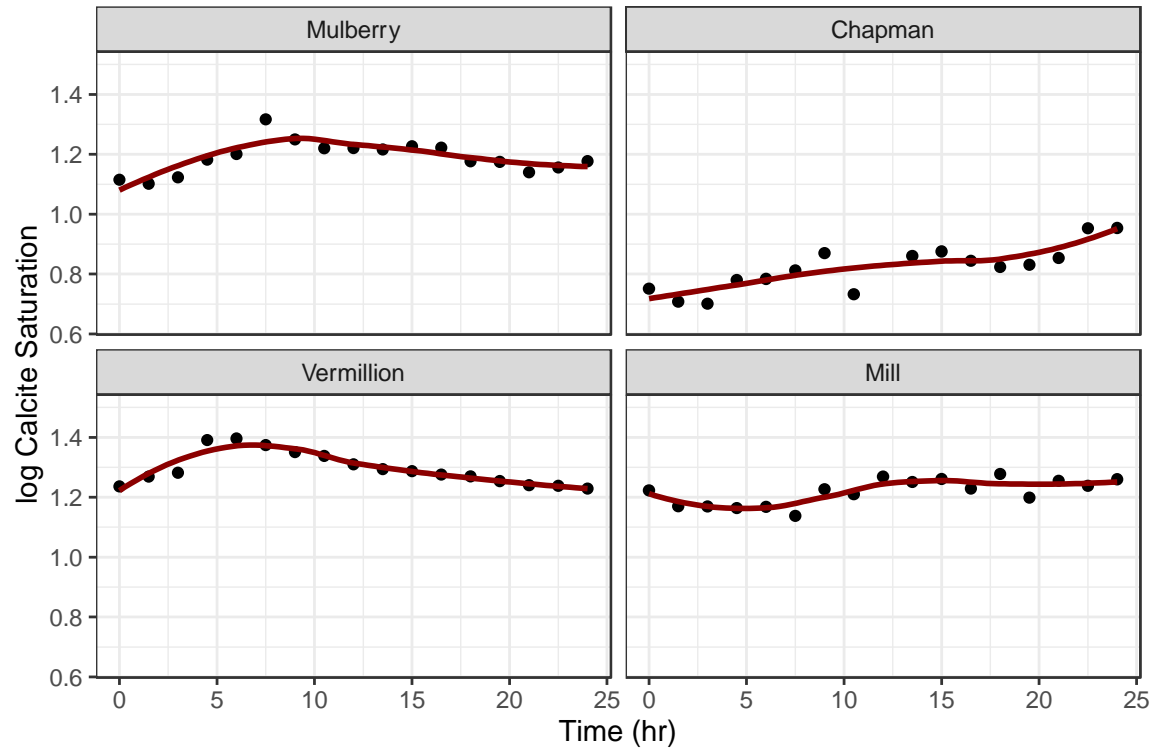
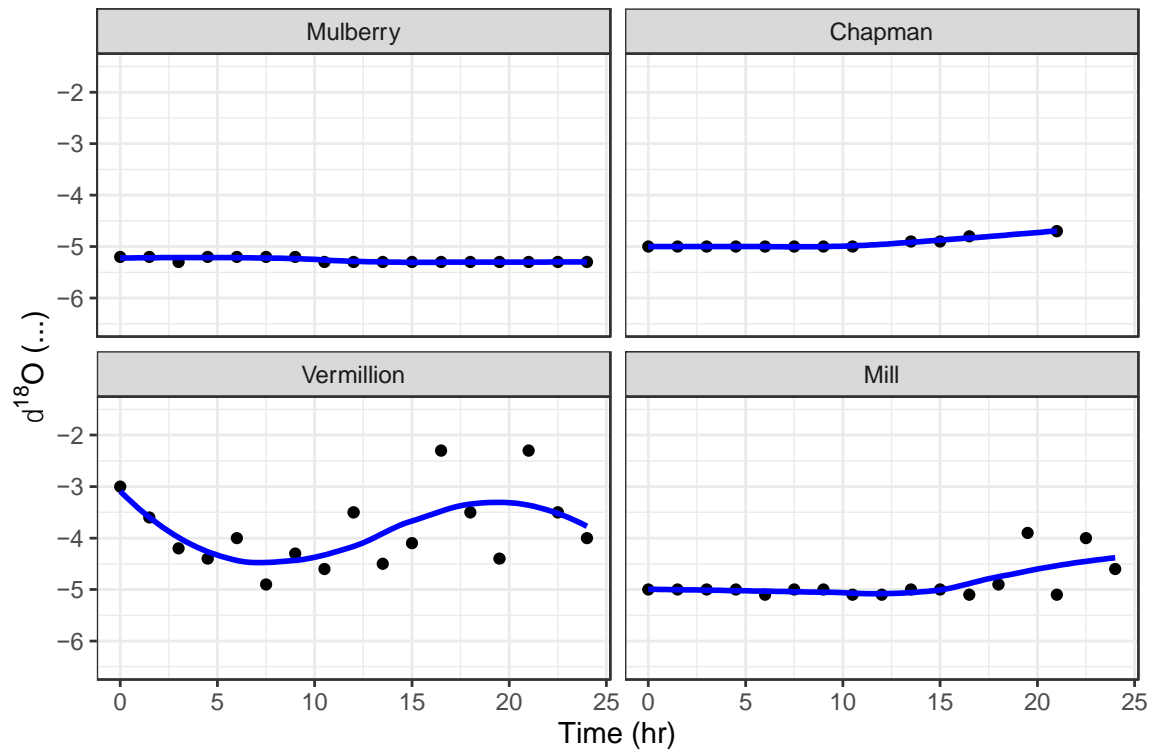
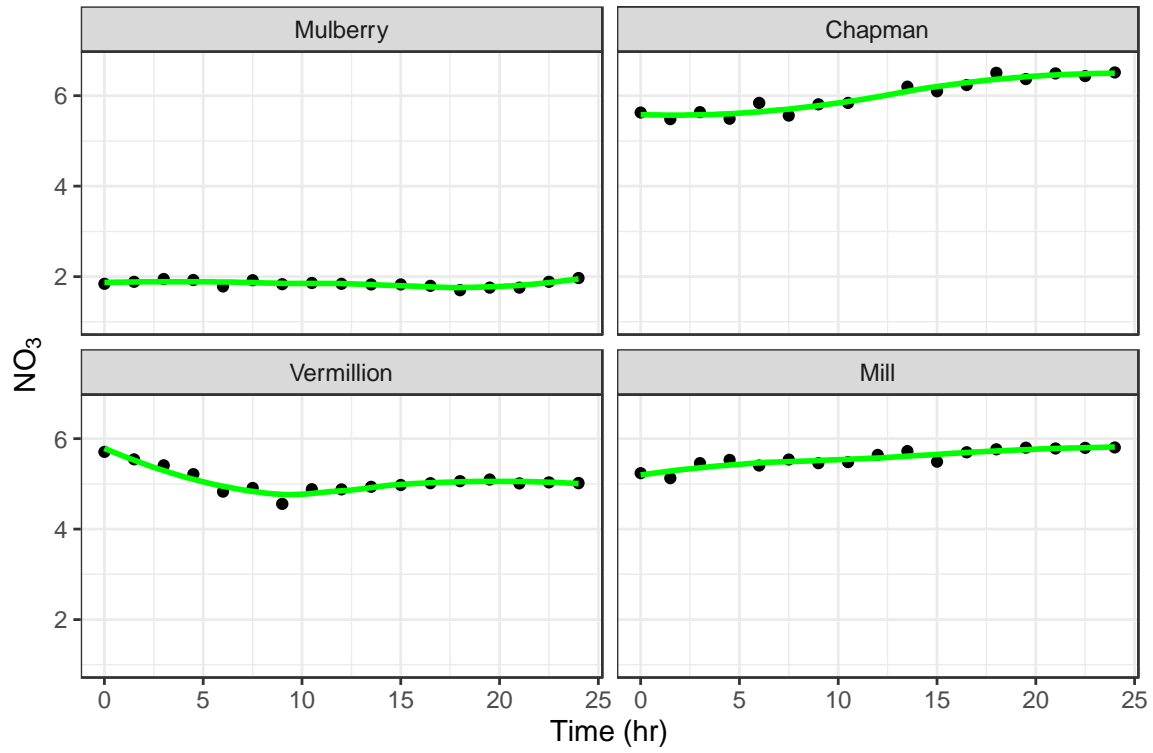


Figure 12 Discharge data over the 24-hour sampling period at each stream.









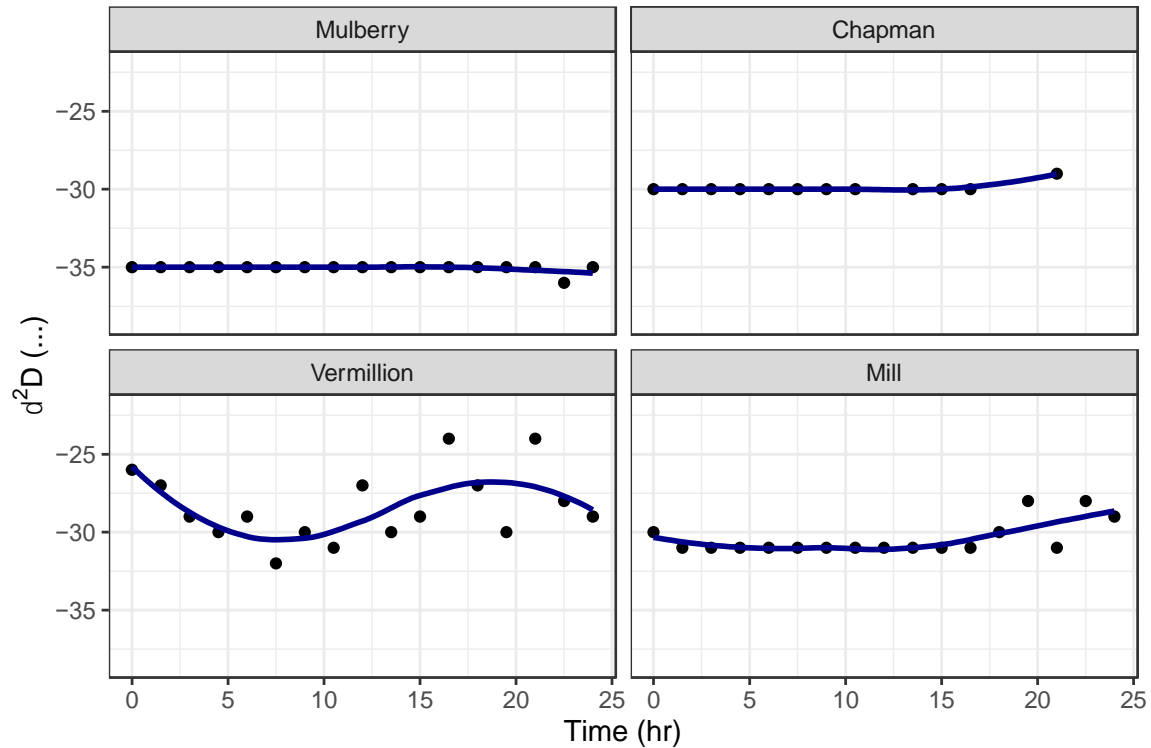


Figure 13 Variations in stream chemistry over 24-hour sampling period. Shaded area indicates samples taken during the night. Diel variations in field measured parameters (pH, T, DO) and calculated parameters (calcite saturation and excess carbon dioxide) are more evident at streams that do not experience large changes in discharge. NPOC at Chapman and Mill demonstrate some diel variation as seen by the peaks in concentrations near the end of the day. NO_3 increased with decreasing discharge at Mill and Chapman. Stable isotopes of water were generally consistent during the day at Mulberry, Chapman and Mill. Mill and Chapman isotopes were slightly higher at night. Vermillion isotopes are a result of diel variations (lower during the day and higher at night).

BFI & Clay vs Chemistry Graphs

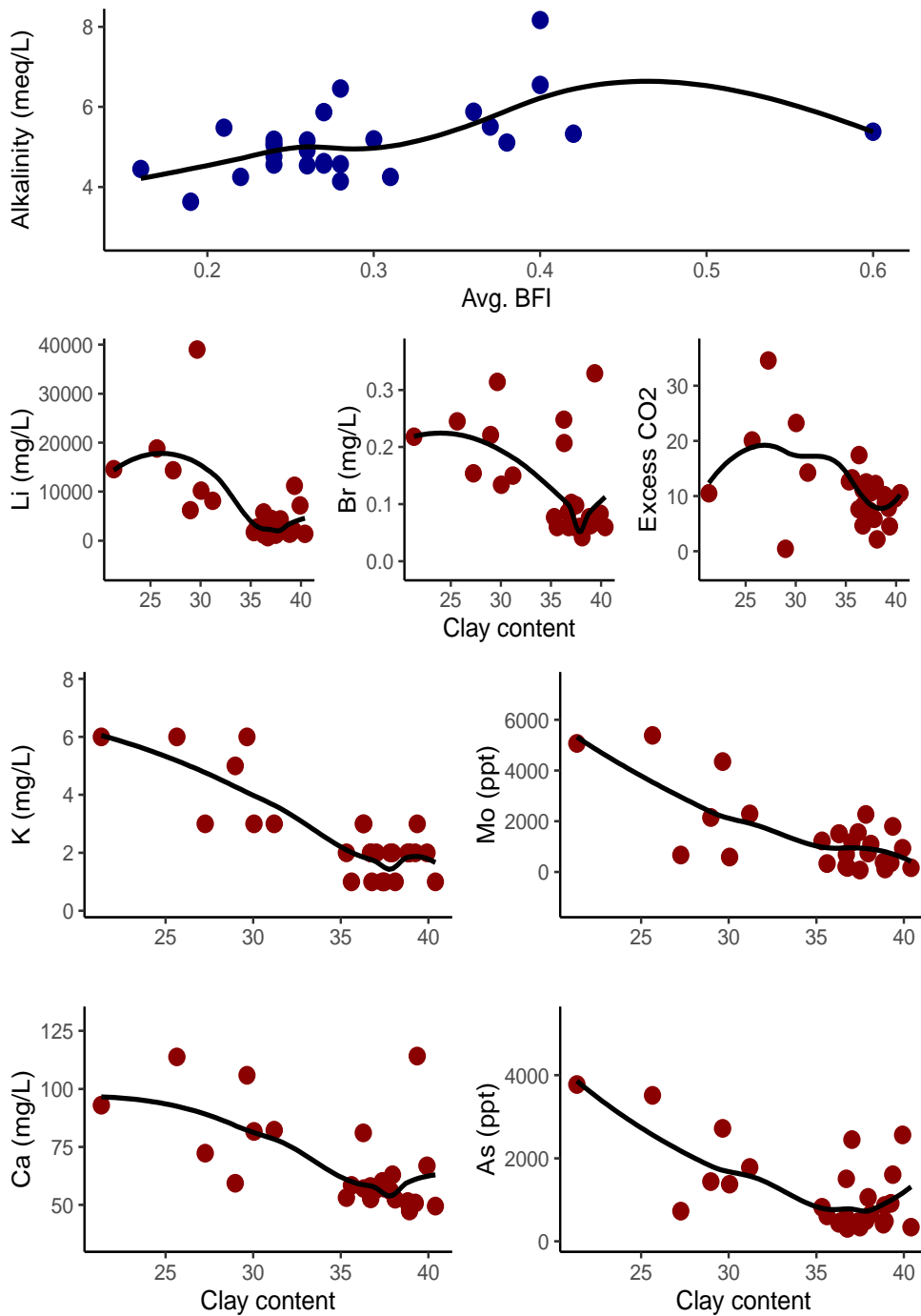


Figure 14 Stream alkalinity increases with groundwater discharge (BFI). Parameters often associated with groundwater discharge (Li, Br, and CO₂) decrease with clay content, possibly indicating that clay limits groundwater discharge. Cations and metals concentrations in streams also are generally lower in watersheds with higher clay content.